NASA/TM-20210015042

Noise Measurements From Ground Tests of the Moog SureFly Vehicle

Dennis L. Huff, Brenda S. Henderson, and Jordan D. Cluts
Glenn Research Center, Cleveland, Ohio

Jeffrey Bennett and Justin Jantzen
Moog, Inc., Loveland, Ohio

May 2021

NASA STI Program . . . in Profile

Since its founding, NASA has been dedicated to the advancement of aeronautics and space science. The NASA Scientific and Technical Information (STI) Program plays a key part in helping NASA maintain this important role.

The NASA STI Program operates under the auspices of the Agency Chief Information Officer. It collects, organizes, provides for archiving, and disseminates NASA's STI. The NASA STI Program provides access to the NASA Technical Report Server—Registered (NTRS Reg) and NASA Technical Report Server—Public (NTRS) thus providing one of the largest collections of aeronautical and space science STI in the world. Results are published in both non-NASA channels and by NASA in the NASA STI Report Series, which includes the following report types:

- TECHNICAL PUBLICATION. Reports of completed research or a major significant phase of research that present the results of NASA programs and include extensive data or theoretical analysis. Includes compilations of significant scientific and technical data and information deemed to be of continuing reference value. NASA counter-part of peer-reviewed formal professional papers, but has less stringent limitations on manuscript length and extent of graphic presentations.

- TECHNICAL MEMORANDUM. Scientific and technical findings that are preliminary or of specialized interest, e.g., "quick-release" reports, working papers, and bibliographies that contain minimal annotation. Does not contain extensive analysis.

- CONTRACTOR REPORT. Scientific and technical findings by NASA-sponsored contractors and grantees.

- CONFERENCE PUBLICATION. Collected papers from scientific and technical conferences, symposia, seminars, or other meetings sponsored or co-sponsored by NASA.

- SPECIAL PUBLICATION. Scientific, technical, or historical information from NASA programs, projects, and missions, often concerned with subjects having substantial public interest.

- TECHNICAL TRANSLATION. English-language translations of foreign scientific and technical material pertinent to NASA's mission.

For more information about the NASA STI program, see the following:

- Access the NASA STI program home page at http://www.sti.nasa.gov

- E-mail your question to help@sti.nasa.gov

- Fax your question to the NASA STI Information Desk at 757-864-6500

- Telephone the NASA STI Information Desk at 757-864-9658

- Write to:
  NASA STI Program
  Mail Stop 148
  NASA Langley Research Center
  Hampton, VA 23681-2199

NASA/TM-20210015042

Noise Measurements From Ground Tests of the Moog SureFly Vehicle

Dennis L. Huff, Brenda S. Henderson, and Jordan D. Cluts
Glenn Research Center, Cleveland, Ohio

Jeffrey Bennett and Justin Jantzen
Moog, Inc., Loveland, Ohio

Prepared for the
2021 AIAA Aviation Forum and Exposition
sponsored by the American Institute of Aeronautics and Astronautics
Virtual Event, August 2–6, 2021

National Aeronautics and
Space Administration

Glenn Research Center
Cleveland, Ohio 44135

May 2021

Acknowledgments

This work was supported by the Revolutionary Vertical Lift Technology (RVLT) project in the Advanced Air Vehicles Program. Thanks to Dr. Paula Dempsey of NASA Glenn Research Center for her help establishing the agreement with Moog, Inc. Also, thanks to the staff of Moog, Inc. for their help conducting and supporting the test. Dr. Robert Dougherty, OPTINAV, provided valuable guidance on the processing of the phased array data. Dr. Christopher Miller, NASA Glenn, conducted flow simulations that were helpful for interpreting the phased array results.

This work was sponsored by the Advanced Air Vehicle Program
at the NASA Glenn Research Center

Level of Review: This material has been technically reviewed by technical management.

Available from

NASA STI Program
Mail Stop 148
NASA Langley Research Center
Hampton, VA 23681-2199

National Technical Information Service
5285 Port Royal Road
Springfield, VA 22161
703-605-6000

This report is available in electronic form at http://www.sti.nasa.gov/ and http://ntrs.nasa.gov/

Noise Measurements From Ground Tests of the Moog SureFly Vehicle

Dennis L. Huff, Brenda S. Henderson, and Jordan D. Cluts
National Aeronautics and Space Administration
Glenn Research Center
Cleveland, Ohio 44135

Jeffrey Bennett and Justin Jantzen
Moog, Inc.
Loveland, Ohio 45140

Abstract

Noise measurements from a ground test of a small vertical lift research vehicle are presented. The proof-of-concept all-electric vehicle called "SureFly" was developed by Moog, Inc. A cooperative effort between NASA and Moog, Inc. has led to one of the first acoustic test datasets from an Urban Air Mobility (UAM) vehicle being developed for passenger and cargo. Results show propeller and possibly motor tones are important for the overall noise levels. The vehicle has four support arms each with a pair of contra-rotating propellers. Noise measurements show higher noise levels from the lower propellers, likely due to inflow distortion from the arms and top propellers. Possible motor noise was identified by calculating harmonics of the line frequency and comparing to the tones in the narrowband acoustic spectra and phased microphone array data. The acoustic far field was found to be about 100 ft away from the vehicle, but additional microphones are needed to provide a better assessment. Results show the presence of modulation for some test conditions. The work reported here is only for ground tests.

Introduction

There is a new exciting research area emerging for small air vehicles designed for short-range package delivery and passenger service. The term "Urban Air Mobility (UAM)" has been coined to describe it, but these vehicles may benefit in a broad range of applications. It is envisioned that small vehicles carrying just a few passengers or cargo would fly short duration missions between "vertiports" and integrate with traditional transportation systems to form a new network of travel options. A motivation for UAM is reducing travel time for congested cities where people spend hours in automobiles during their commute to and from work.

Aircraft noise research has historically focused on communities surrounding airports. The introduction of UAM vehicles will increase air traffic away from airports. The response to UAM operations in and around these communities is unknown. A recent white paper from Uber Elevate (Ref. 1) includes a discussion on community noise. Research is just beginning for assessing noise levels and determining appropriate metrics for judging annoyance. NASA has formed an Urban Air Mobility Noise Working Group (UNWG) to help coordinate the research and raise awareness across government agencies, universities and industry worldwide. A white paper (Ref. 2) was published recently that identifies technology needs, gaps and priorities in four areas: noise prediction tools and technologies, ground and flight testing, human response and metrics, and regulation/policy (led by the FAA). A common need across all areas is for acoustic data from representative UAM vehicles to begin characterizing the sound, enabling validation of prediction codes, and understanding which sources are most important for reducing noise.

As a part of NASA's Revolutionary Vertical Lift Technology (RVLT) Project, a partnership was established between NASA and Moog, Inc. (formerly Workhorse) to measure noise from a research vehicle called "SureFly." In November 2019, the first set of acoustic measurements were obtained for the vehicle during ground run-ups. Subsequent tests will include hover and flyovers with the SureFly all-electric vehicle and a newer hybrid-electric propulsion vehicle. The purpose of this paper is to present results from the initial ground tests. Assessments have been made to determine the acoustic far field distance and characterize the noise from combinations of single and multiple rotors operating over a range of speeds. An initial assessment of motor noise has also been included.

SureFly Vehicle and Experimental Setup

The Moog Surefly proof-of-concept all-electric research vehicle is pictured in Figure 1. There are four arms with eight contra-rotating rotors providing lift, with a differential speed control driving the independent motors. The payload of this vehicle is 550 lb. It uses advanced fly-by-wire flight controls with stability augmentation and autopilot capabilities. Lithium Ion batteries provide continuous power, for a yet to be defined flight time. Eight Emrax air-cooled electric motors operate at up to 18 kW each using liquid-cooled inverters. The research vehicle used 92-in. diameter, fixed-pitch composite propellers manufactured by Sterna Aircraft LLC. Note that propeller and rotor are used interchangeably in this paper. Likely sources of noise include the propellers (including interaction effects), cooling system fans, cooling system pumps, and electric motors. This proof-of-concept vehicle has not been optimized for noise. The preliminary tests reported here were only meant to characterize the noise and help develop ongoing experimental procedures for acoustic measurements.

Tests were conducted at the Lunken Municipal Airport in Cincinnati, Ohio. Eight G.R.A.S. 67AX ground microphones were positioned as shown in Figure 2 and Figure 3. There were two radial lines of four microphones located directly forward of the vehicle at 0 degrees and portside at –45 degrees. Distances of 25, 50, 100, and 200 ft were chosen to successively double the microphone distance from the origin shown in Figure 3, thereby helping to identify the acoustic far field using spherical spreading roll-off. A National Instruments system was used for data acquisition. The data were acquired at a sampling rate of 50 kHz. Microphone sensitivities were accounted for in the processed data.

Figure 1.—Moog, Inc. SureFly proof-of-concept all-electric research vehicle.

A phased microphone array was placed directly portside and 42 ft away on a 6-ft-high tripod for checkout tests performed on November 5, 2019. The phased array was an ACAM 100 manufactured by the Signal Interface Group (SIG) with BeamformX software written by OptiNav, Inc. (Ref. 3). Analysis of initial data showed reflections from the fuselage and was difficult to interpret. The array was moved to a foam pad on the ground for the second day of testing, as shown in Figure 2. The array was located 21 ft from the left front motors, which was estimated to be an appropriate trade between downwash scrubbing noise and array resolution.

Figure 2.—SureFly vehicle and instrumentation.

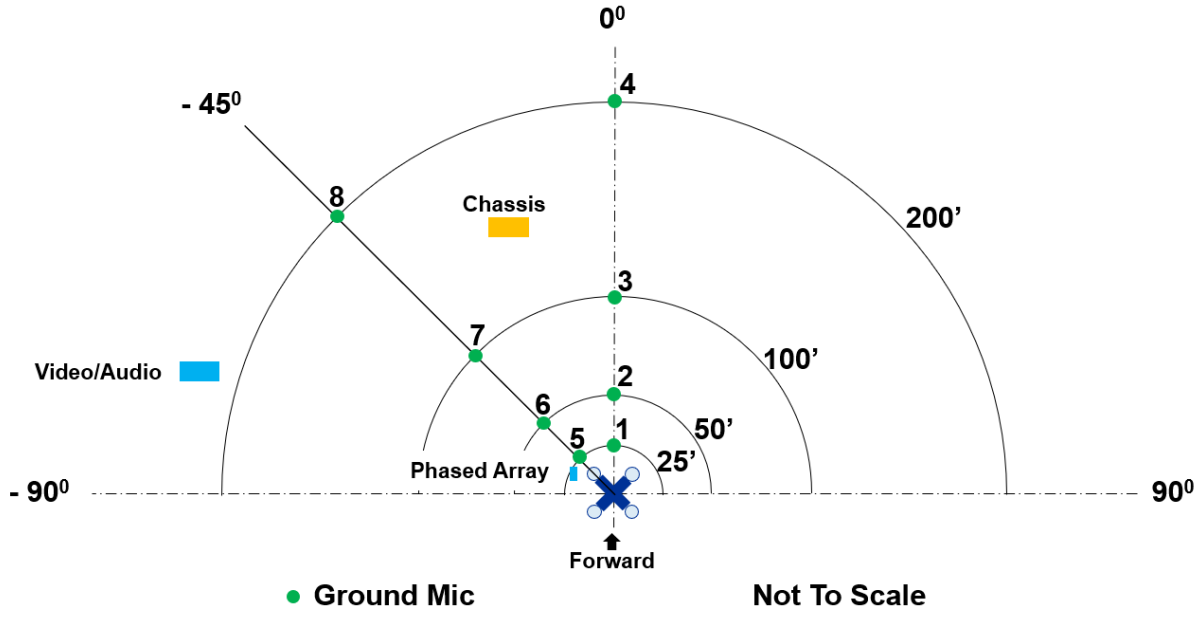

Figure 3.—Location of ground microphones and equipment.

The vehicle was placed on an asphalt surface facing easterly approximately 53 degrees from North (Figure 4). A Hobo U30 weather station was mounted on a tripod approximately 10 ft above the ground. Wind direction, speed, gust amplitudes, relative humidity and temperature were recorded every 10 min during the tests. The vehicle was located so that the origin of the microphone array aligned with the intersection of the four arms supporting the motors and propellers. Figure 5 shows the location of the origin and the coordinate system. Table 1 lists the locations of each propeller hub. Note that the distances reported in the acoustic results are relative to the origin, so the sound sources are at different distances to the microphones depending on the specific propeller and motor location. The information in Table 1 can be used to calculate the distance from each sound source to the microphones.

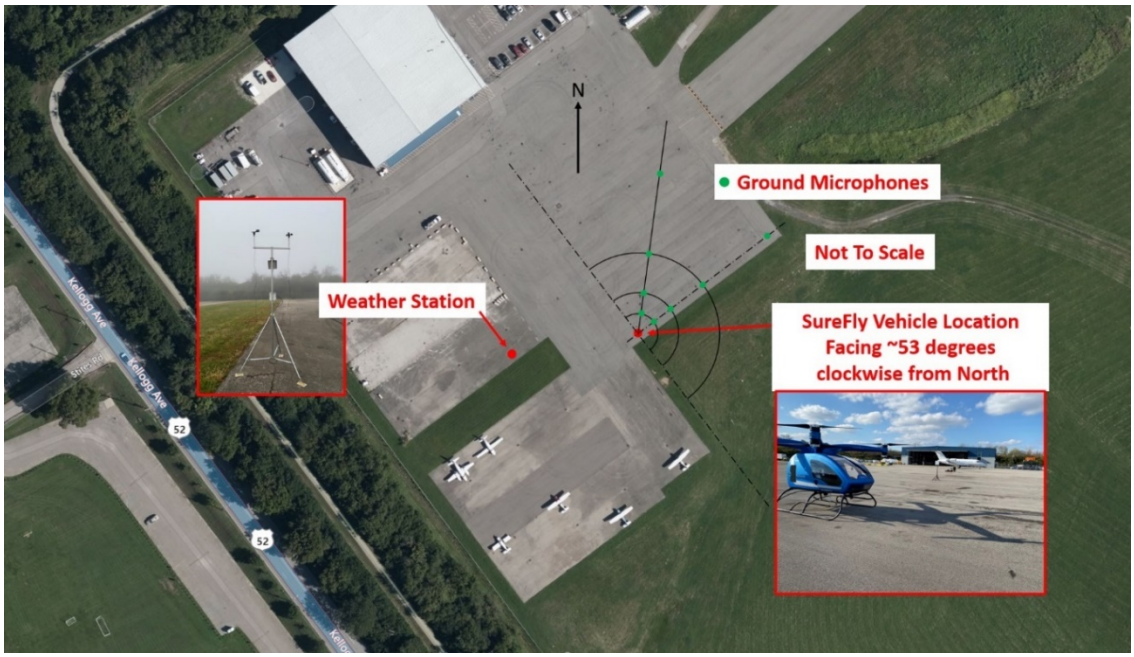

Figure 4.—Aerial view of instrument and SureFly vehicle ground test locations.

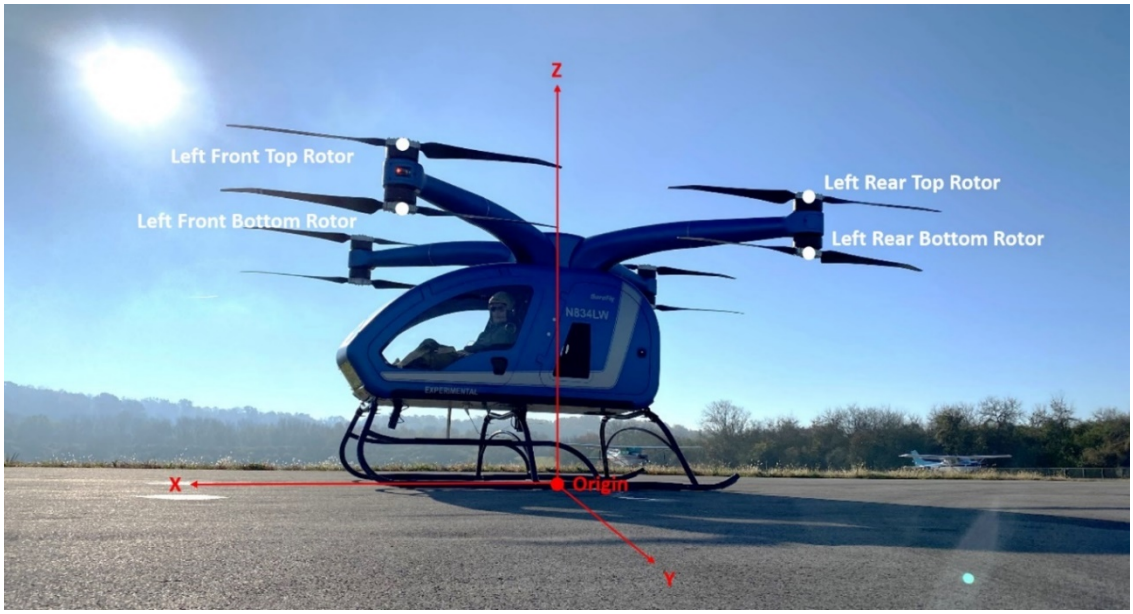

Figure 5.—Origin and coordinate system for locating propeller hubs.

TABLE 1.—ROTOR HUB LOCATIONS, ROTOR NUMBERS AND DIRECTION OF ROTATION

Rotor, (Number)	Direction of rotation, (Viewed from top)	X, (ft)	Y, (ft)	Z, (ft)
Left Front Top Rotor (2)	clockwise	5.313	5.313	8.117
Left Front Bottom Rotor (5)	counterclockwise	5.313	5.313	6.677
Left Rear Top Rotor (3)	counterclockwise	–5.313	5.313	8.117
Left Rear Bottom Rotor (8)	clockwise	–5.313	5.313	6.677
Right Front Top Rotor (1)	counterclockwise	5.313	–5.313	8.117
Right Front Bottom Rotor (6)	clockwise	5.313	–5.313	6.677
Right Rear Top Rotor (4)	clockwise	–5.313	–5.313	8.117
Right Rear Bottom Rotor (7)	counterclockwise	–5.313	–5.313	6.677

Results

Tests were performed during the morning of November 6, 2019. Data were acquired from approximately 9:30 am through 11:15 am, with specific times selected between other air traffic disturbances. Ground run-ups were done at 20, 35, 45, and 55 percent motor speeds. The shaft speeds for each motor were recorded by a vehicle data acquisition system. A rotational speed of 2100 rpm was designated as 100 percent speed and the percent speeds used in this paper represent an average over the eight rotors. The vehicle lifted off at approximately 57 percent speed, so 55 percent speed was chosen as the highest power for these ground tests. Data for 20 percent speed were not processed as this speed was deemed to be too low to be a concern for noise. The first set of tests were done with all rotors operating and the test pilot holding motor speeds for at least 20 s to acquire acoustic data.

Data were acquired for various combinations of rotors operating as shown in Table 2. The combinations include Left Front Top Rotor (B), Left Front Bottom Rotor (C), Left Front Both Rotors (D), Left Rear Top Rotor (E), Left Rear Bottom Rotor (F), Left Rear Both Rotors (G), and All Rotors (A, H). The times listed in the table are approximate. Acoustic data files stored from these tests are labeled "SureFly_11062019_*runnumber*_Slot2_ai*X*," where the run number is listed in Table 2 and *X* is the microphone number shown in Figure 3 minus 1 (the microphone numbering starts at 0 instead of 1).

Unfortunately, the data from the weather station was not stored. Table 3 shows data from the Lunken Municipal Airport for the morning of the test day (Ref. 4). Tests were delayed in the morning due to fog and low temperatures. No condensation was observed on the test instrumentation.

Figure 6 shows how the rpm for each rotor varies with time for data set H with all propellers operating. The direction of rotation for each rotor is indicated in the legend of the figure with CCW for counterclockwise and CW for clockwise. The top rotors are designated 1 through 4 and the bottom rotors are numbered 5 through 8. Note the speeds are different for each rotor as prescribed by the controller for thrust balance. Plots of rpm versus time for each test condition are included in Appendix A (Figure 28 to Figure 35).

Sound pressure level spectra for each ground microphone are shown in Figure 7 with all rotors operating at 35 percent speed. Ambient noise spectra are included for microphones 4 and 8, which were acquired with no rotors operating. As expected, the sound level drops for microphones further away from the vehicle. For microphones located 200 ft away, the ambient levels are close enough to the vehicle measurements to be a concern, particularly at higher frequencies. The lower plots show the spectra from 0 to 2 kHz and reveal the expected harmonics of the propeller tones. The tones near 800 Hz are believed to be from the motors and will be discussed later. The directivity in the near field at 0 and –45 degrees is similar.

TABLE 2.—DATA LOG

Test condition	Time, (EST)	Speed, (Percent)	Run number	Phased array record	Comments
No Rotors	9:34 AM	0	0001, 0002	--------	Ambient
	----------	--------	----------	--------	----------
A-All Rotors (1-8)	9:54 AM	20	0003, 0004	2,3	Use 0004, do not use 0003 for array
----------	9:55 AM	35	0005	4	----------
----------	9:56 AM	45	0006	5	----------
----------	9:57 AM	54 to 55.5	0007	6	Almost liftoff
----------	----------	----------	----------	--------	----------
----------	----------	0	0008	7	Ambient
----------	----------	----------	----------	--------	----------
B-Left Front Top Rotor (2)	10:04 AM	20	0009, 0010	8	Use 0010
----------	10:06 AM	35	0011	9	----------
----------	10:06 AM	45	0012,0013	10	Use 0013
----------	10:08 AM	55	0014	11	----------
----------	----------	----------	----------	--------	----------
C-Left Front Bottom Rotor (5)	10:20 AM	20	0015-17	12	Use 0017
----------	10:21 AM	35	0018	13	----------
----------	10:22 AM	45	0019	14	----------
----------	----------	55	0020	15,16	Do not use 15
----------	----------	----------	----------	--------	----------
D-Left Front Both Rotors (2 and 5)	10:29 AM	20	0021-25	17	Use 0025
----------	10:30 AM	35	0026	18	----------
----------	10:31 AM	45	0027	19	Heard modulation
----------	10:32 AM	55	0028	20	----------
----------	----------	----------	----------	--------	----------
E-Left Rear Top Rotor (3)	10:41 AM	20	0029	21	----------
----------	10:43 AM	35	0030	22	----------
----------	10:44 AM	45	0031,0032	23	----------
----------	10:51 AM	55	0033	24,25	Use 25
----------	----------	----------	----------	--------	----------

TABLE 2.—(Concluded)

Test condition	Time, (EST)	Speed, (Percent)	Run number	Phased array record	Comments
F-Left Rear Bottom Rotor (8)	10:53 AM	20	0034	26	----------
----------	11:00 AM	35	0035	27,28	Use 28
----------	11:01 AM	45	0036	29	----------
----------	11:02 AM	55	0037	30	----------
----------	----------	----------	----------		----------
G-Left Rear Both Rotors (3 and 8)	11:05 AM	35	0038	31	----------
----------	11:06 AM	45	0039	32	Heard modulation
----------	11:07 AM	55	0040	33	No modulation
----------	----------	----------	----------		----------
H-All Rotors (1-8)	11:10 AM	35	0041	34	----------
----------	----------	45	0042	35	----------
----------	11:14 AM	55	0043, 0044	36	Use 0044
----------	----------	----------	----------	--------	----------
----------	11:15 AM	0	0045	37,38	Ambient, Use 38

TABLE 3.—WEATHER DATA FOR NOVEMBER 6, 2019

Time	Temperature	Dew Point	Humidity	Wind	Wind Speed	Wind Gust	Pressure	Precip.	Condition
8:53 AM	35 °F	34 °F	96 %	CALM	0 mph	0 mph	29.95 in	0.0 in	Fog
9:03 AM	35 °F	34 °F	96 %	CALM	0 mph	0 mph	29.95 in	0.0 in	Mostly Cloudy
9:15 AM	36 °F	36 °F	100 %	CALM	0 mph	0 mph	29.95 in	0.0 in	Partly Cloudy
9:53 AM	40 °F	37 °F	89 %	CALM	0 mph	0 mph	29.93 in	0.0 in	Fair
10:53 AM	49 °F	36 °F	61 %	VAR	3 mph	0 mph	29.91 in	0.0 in	Fair
11:53 AM	52 °F	35 °F	53 %	VAR	7 mph	0 mph	29.89 in	0.0 in	Fair

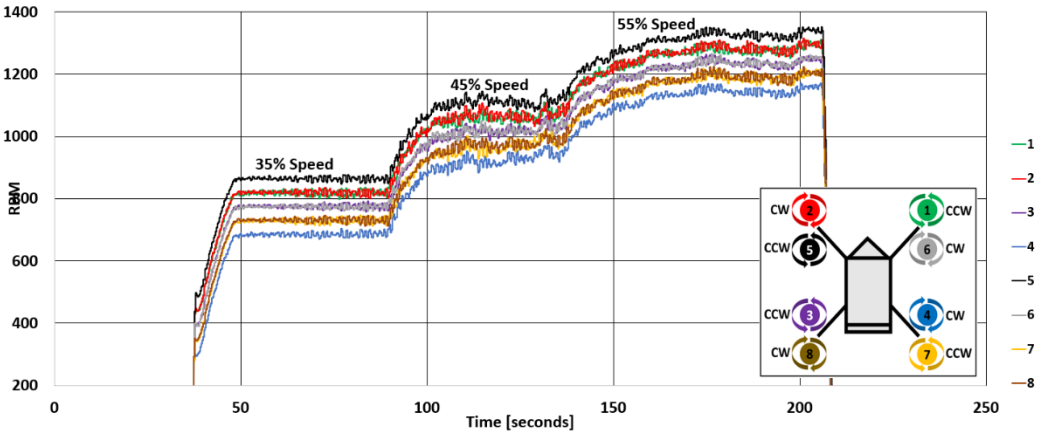

Figure 6.—Rotor speed versus time for each of the eight propellers, test condition H. From highest to lowest speed, the motors are: 5, 1 and 2, 3 and 6, 7 and 8, 4.

Spectra for 45 and 55 percent motor speeds are shown in Figure 8 and Figure 9, respectively. As expected, the sound levels increase with motor speed and the propeller harmonics shift to higher frequencies. At higher motor speeds, multiple peaks of propeller tones are observed. This is from the rotors operating at different speeds as shown in Figure 6. During the test, a modulation sound was observed that is due to the rotors operating at slightly different speeds.

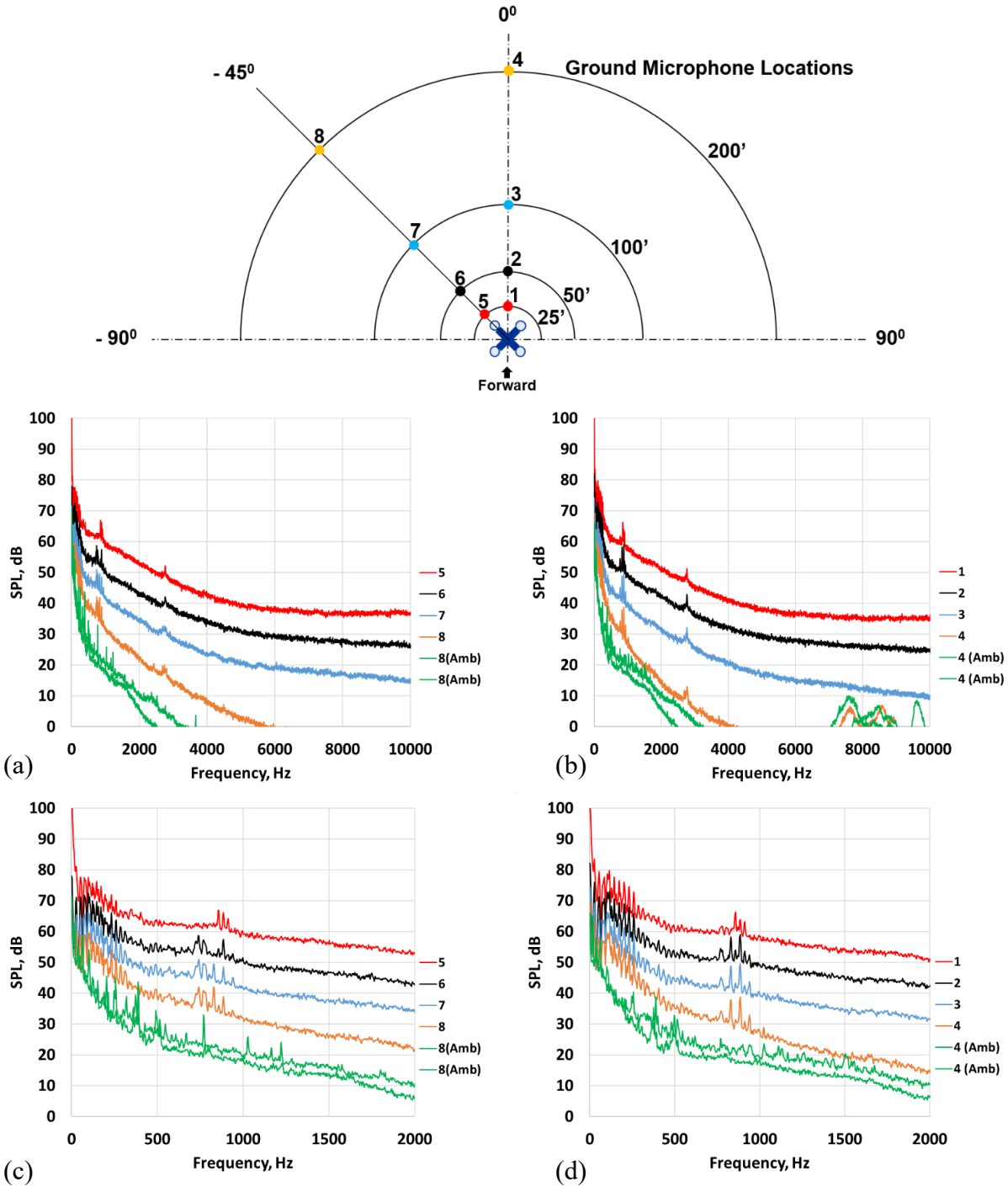

Figure 7.—SPL for all rotors, 35 percent speed, run number 0041. (a) –45 degrees, 0 to 10 kHz. (b) 0 degrees, 0 to 10 kHz. (c) –45 degrees, 0 to 2 kHz. (d) 0 degrees, 0 to 2 kHz.

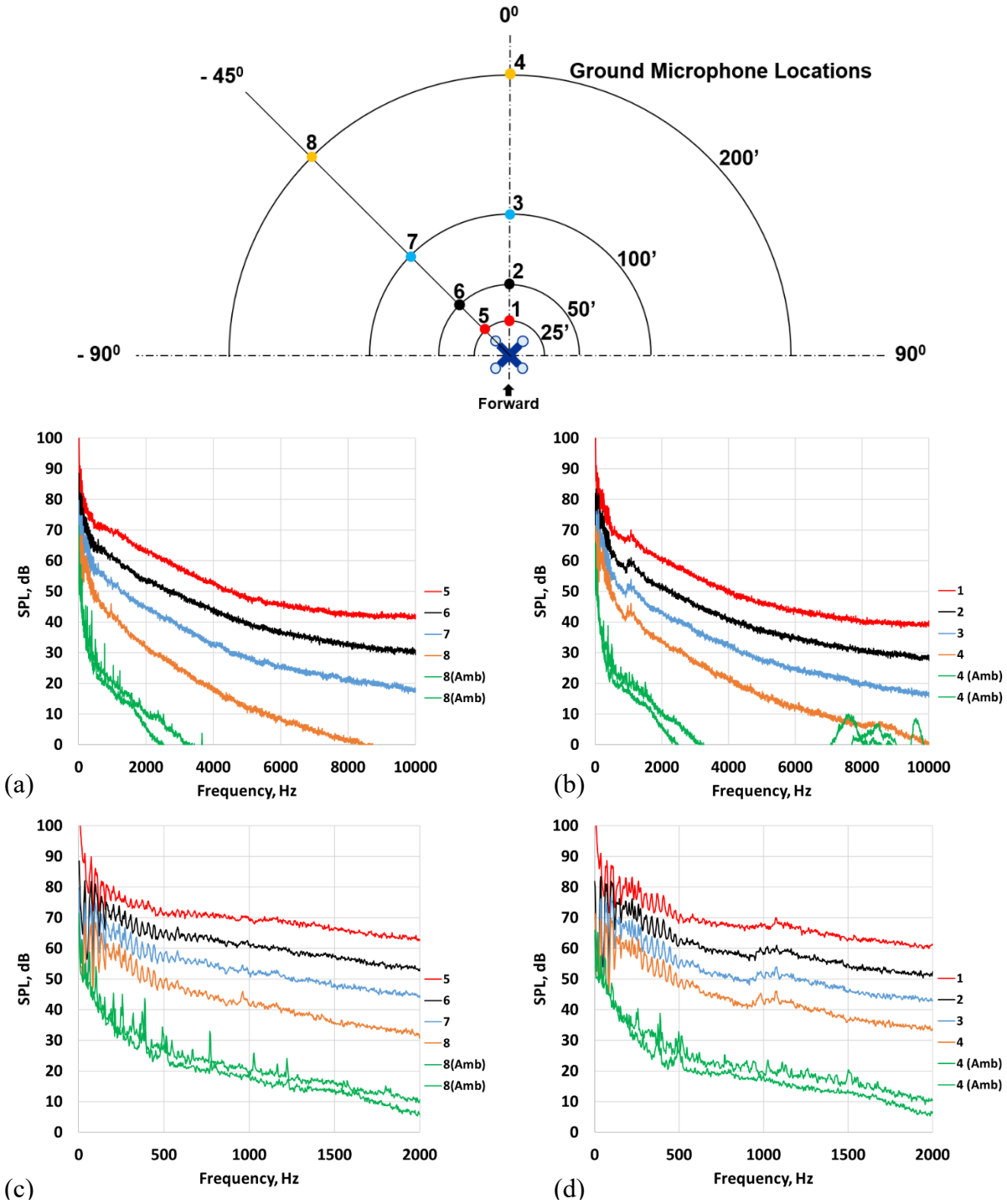

Figure 8.—SPL for all rotors, 45 percent speed, run number 0042. (a) –45 degrees, 0 to 10 kHz. (b) 0 degrees, 0 to 10 kHz. (c) –45 degrees, 0 to 2 kHz. (d) 0 degrees, 0 to 2 kHz.

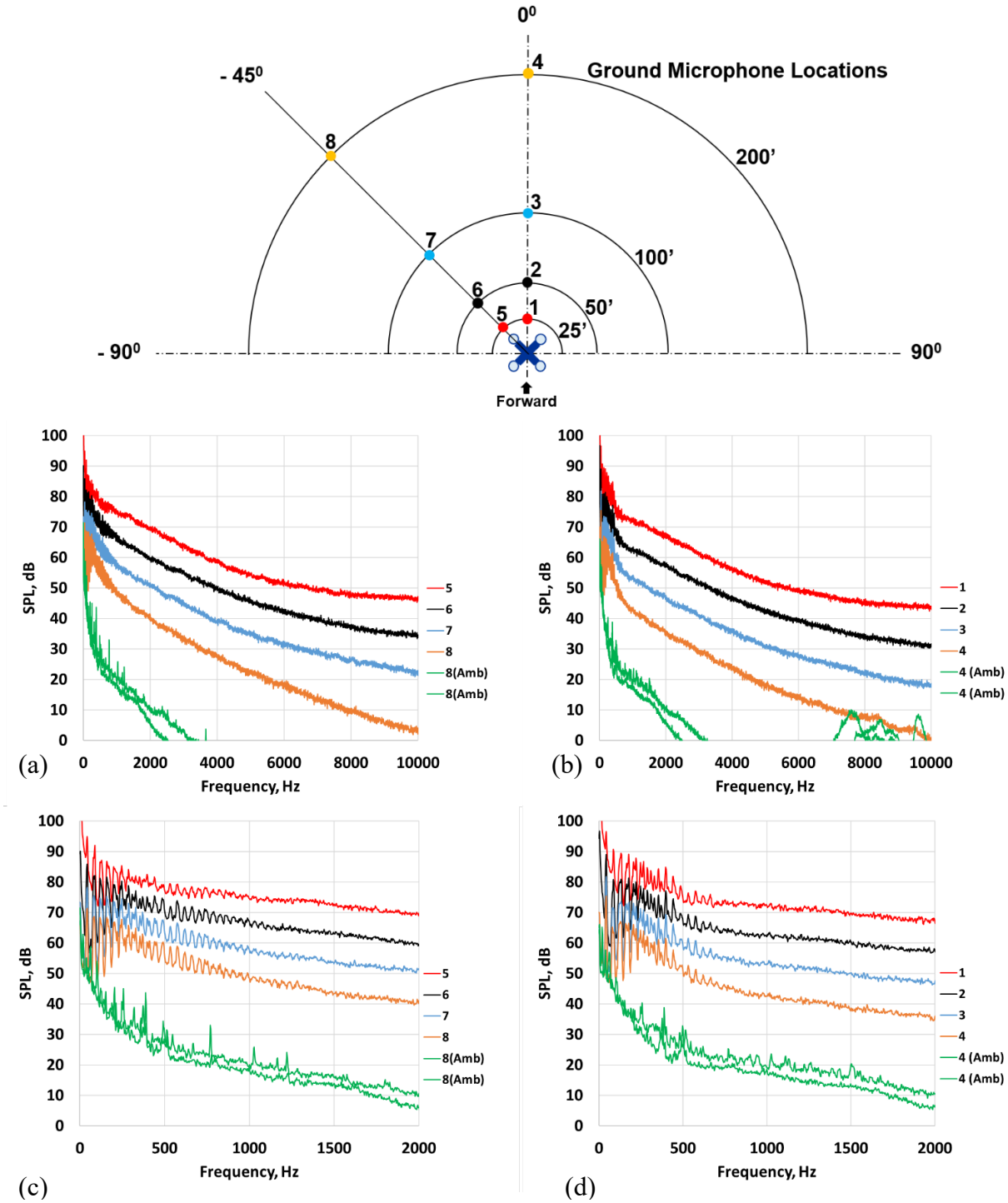

Figure 9.—SPL for all rotors, 55 percent speed, run number 0044. (a) –45 degrees, 0 to 10 kHz. (b) 0 degrees, 0 to 10 kHz. (c) –45 degrees, 0 to 2 kHz. (d) 0 degrees, 0 to 2 kHz.

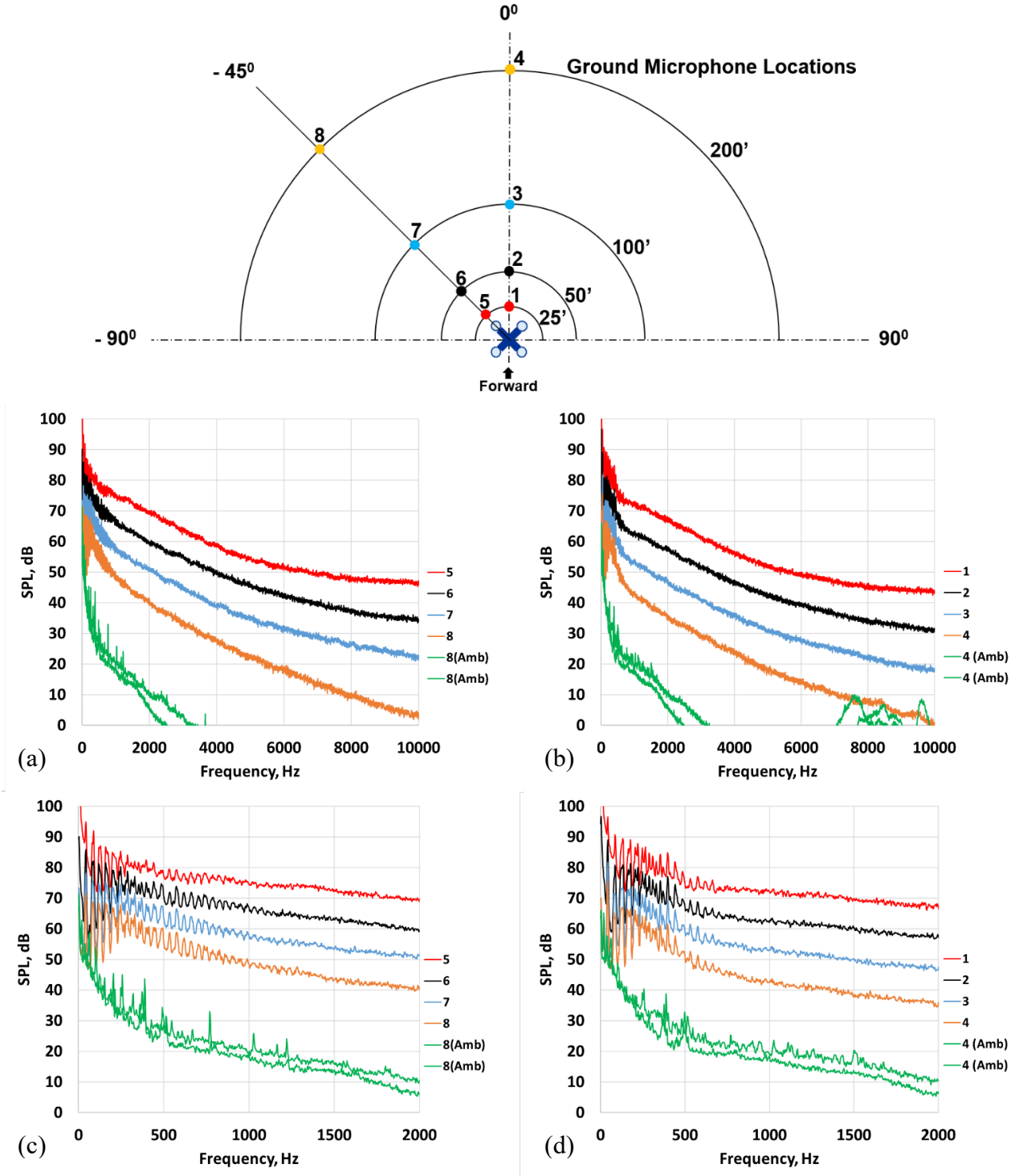

Figure 10.—SPL for left front top rotor, 45 percent speed, run number 0013. (a) –45 degrees, 0 to 10 kHz. (b) 0 degrees, 0 to 10 kHz. (c) –45 degrees, 0 to 2 kHz. (d) 0 degrees, 0 to 2 kHz.

For comparison, the spectra for only the left front top rotor operating at 45 percent speed is shown in Figure 10. The tones are more distinct with only one rotor and motor operating. The modulation that was observed with multiple rotors is absent. Acoustic spectra for all test conditions and speeds are included in Appendix B (Figure 37 to Figure 57).

The modulation that was observed with two rotors is likely from the tones of the blade passing frequencies and harmonics with slightly different speeds. A pulse function can be described by

$$f(t) = Acos(\omega_1 t + \varphi_1) + (A + \Delta A)\cos(\omega_2 t),$$

where ω_1 is a frequency for a tone with amplitude A, ω_2 is a frequency for a tone with an amplitude of $(A + \Delta A)$, and φ_1 is the difference in the phase angles at time $t = 0$. Let $\tilde{\varphi} = \pi + \varphi$, so

$$f(t) = (A + \Delta A)\sin(\omega_2 t) - Asin(\omega_1 t + \tilde{\varphi}).$$

Using the identity $\sin(x) - \sin(y) = 2\cos\left(\frac{x+y}{2}\right)\sin\left(\frac{x-y}{2}\right)$,

$$f(t) = 2A\left[sin\left(\frac{\omega_2-\omega_1}{2}t - \frac{\tilde{\varphi}}{2}\right)cos\left(\frac{\omega_2+\omega_1}{2}t + \frac{\tilde{\varphi}}{2}\right)\right] + \Delta Acos(\omega_2 t).$$

The first term in this equation can be used to calculate the modulation beat frequency. This assumes the propagation distance is the same for both rotors. For the rotors operating on the left front arm at 45 percent (average) speed, the blade passing frequency is 34.4447 Hz for the top rotor and 35.9242 Hz for the bottom rotor, the difference of which is the beat frequency of 1.4795 Hz. The actual speeds for the rotors are plotted in Figure 31. The amplitude of sound from the bottom rotor is roughly twice that from the upper rotor (a little over 6 dB and assuming some coherence between sound radiating from upper and lower rotor), so $A = 1$ and $\Delta A = 1$. The resulting waveform is shown in Figure 11.

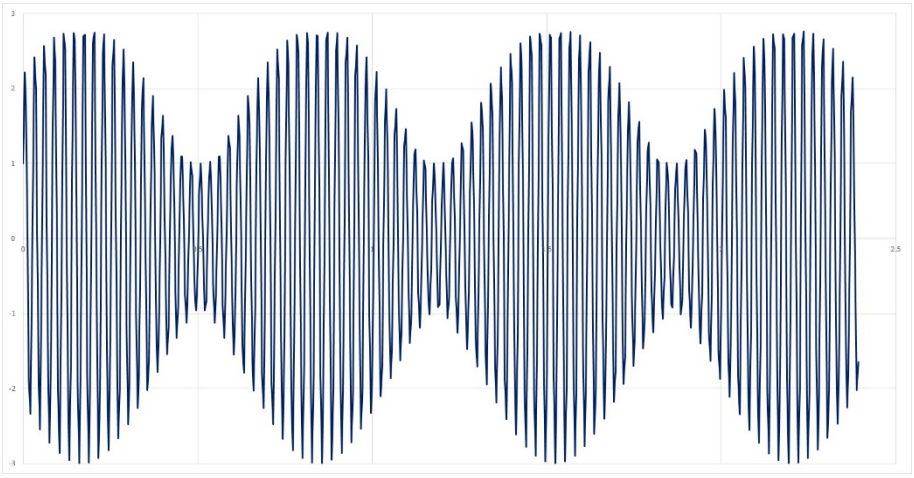

Figure 11.—Modulation waveform simulation for two rotors with blade passing frequencies of 34.4447 Hz and 35.9242 Hz with an amplitude difference of 6 dB.

The spectra are overlayed in Figure 12. The double peaks associated with the two different rotor speeds are shown and the modulation will likely only occur for the lower harmonics as the disparity in frequency between the two rotor speeds increases with harmonic number and beating only occurs when the two frequencies are close in value. Also, the difference in the amplitudes of the tones between the top and bottom rotor is larger for higher harmonics.

The beat frequencies for some of the higher blade passing frequency harmonics were computed and are shown in Table 4.

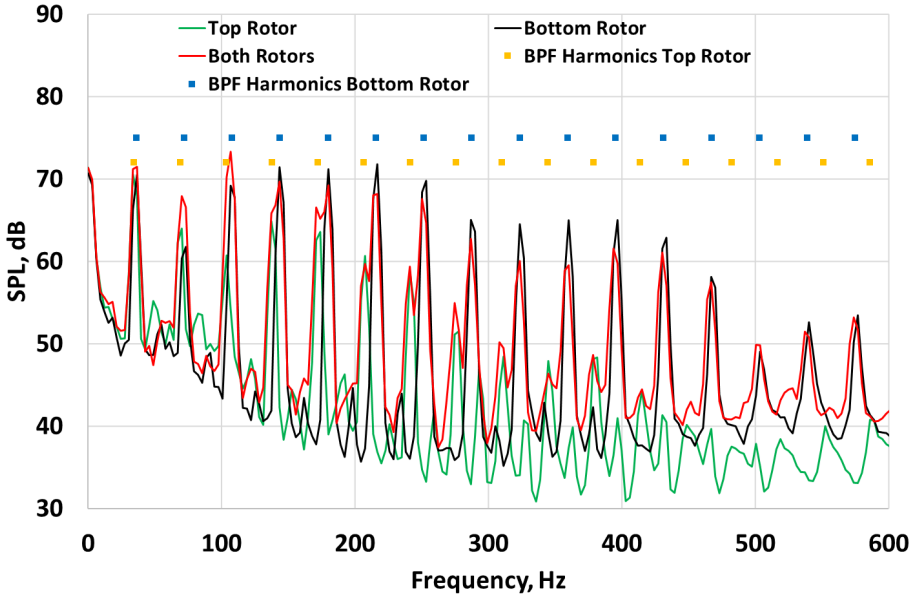

Figure 12.—Spectra for left front rotors, 45 percent average speed, blade passing harmonics for each rotor are indicated, microphone 3.

TABLE 4.—BEAT FREQUENCIES FOR HARMONICS OF THE BLADE PASSING FREQUENCIES FOR LEFT FRONT ROTORS, 45 PERCENT AVERAGE SPEED

BPF harmonic, Hz	Beat frequency, Hz
1	1.48
2	2.95
3	4.43
4	5.91
5	7.38

Since the motors have not been tested in isolation, it is not possible to definitively identify motor tones in the acoustic spectra. The possibility of motors tones can be inferred by calculating the electrical line frequencies. The electrical line frequencies are calculated knowing the number of pole pairs (10) times the rpm divided by 60. Depending on the controller, this frequency and higher harmonics can excite motor tones. Figure 13 shows that harmonics at 6 and 7 times the line frequency are present in the spectra for 55 percent speed. Harmonics of the line frequencies were also observed at 35 and 45 percent motor speeds.

The phased microphone array was used to help separate sound sources. The array was placed on the ground on a foam pad approximately 21 ft (12.8 m) from the left front motors. Buffeting and high broadband noise levels in the acoustic spectra indicate this location was in the downwash from the left front propellers. The investigation was switched to the left rear propellers, at a greater distance, to avoid this problem. Figure 14 shows the acoustic spectrum from one of the flush-mounted microphones on the phased array for the case with only the top rotor operating. The results are qualitatively similar to Figure 13 with both low frequency (<1000 Hz) propeller harmonics and a higher frequency tone at 6 times the line frequency. Note that the bandwidth for the spectra from the phased array is 12.2 Hz.

The aperture for the SIG array limits the ability to resolve sources at low frequencies. For example, the minimum source separation distance is about 15 in. at 1000 Hz, and about 8 in. at 2000 Hz. In addition, there is flow from the propeller that will refract the apparent location of the source.

A 20 s sample was recorded for each test condition. During playback for processing the data, unsteadiness was observed in the beamforming images. Experience with the same phased array in a lab using smaller propellers and motors showed less unsteadiness in the results (Ref. 5). The laboratory results showed a distinct single source for tones that were attributed to the motor and a distributed source for higher frequency propeller broadband noise.

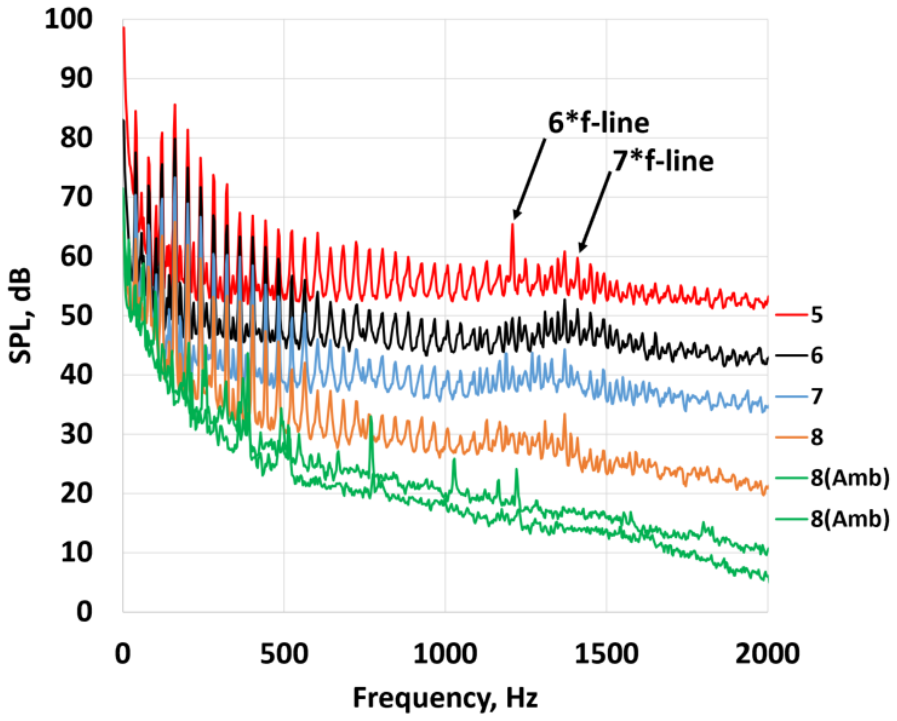

Figure 13.—Motor noise tones for 55 percent motor speed, left rear top rotor, –45 degrees, multiples 6 and 7 of the line frequency are noted.

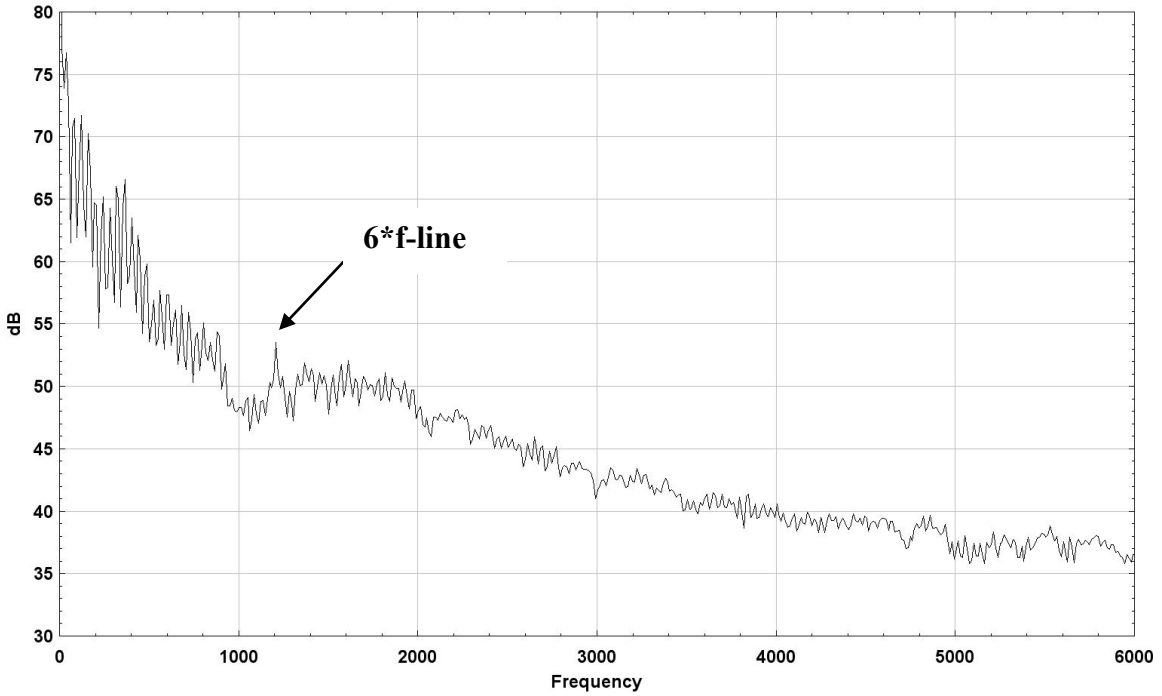

Figure 14.—Phased array for 55 percent motor speed, left rear top rotor.

Figure 15 shows the beamforming image for the tone at 6 times the line frequency (1208 Hz), which is presumed to be from the motor. The image does not directly line up with the motor, but looks similar to motor tones observed in the lab. A flow simulation of the downwash from the rotors and resulting flow over the phased array microphones shows an offset of this amount is possible due to refraction of the acoustic waves.

Figure 16 shows the propeller broadband noise at 4585 Hz. The expected distributed source appears with higher levels coming from the advancing side of the rotor and looks similar to results observed in a laboratory (Ref. 5). This frequency was arbitrarily chosen and results for other frequencies look similar for propeller broadband noise.

The BeamformX software includes a partition feature that helps with source separation. Figure 17 shows three partitions added to distinguish spectra from the advancing side of the propeller (left), the center region that includes the hub and motor, and the retreating side (right). Figure 18 shows the spectra from each region and the total. The total is similar to the spectra shown in Figure 14. For the tone at 1208 Hz, the center partition containing the motor and hub shows the highest contribution to the total. For higher frequencies where the propeller broadband noise is evident, the advancing blade partition has levels that are higher than the retreating side. Since the propeller tip passes through the center partition for a portion of the blade rotation, some contribution from propeller noise is expected. In addition, refraction of the source from the downwash complicates the interpretation of the partitioned results. Future tests should include runs with just the motor to verify the beamform imaging without flow. With these caveats in mind, the results support that there could be a strong contribution from the region containing the motor at 1208 Hz.

Figure 15.—Phased array beamforming image for 55 percent motor speed, left rear top rotor, 1208 Hz.

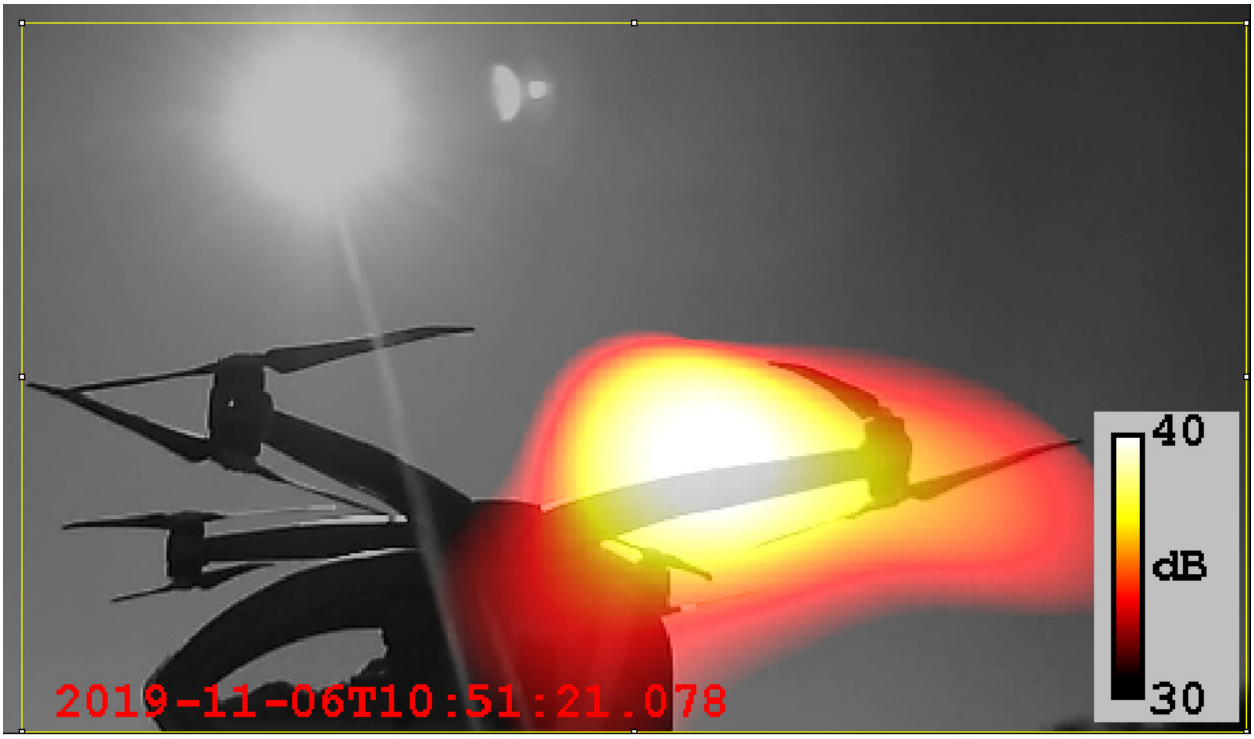

Figure 16.—Phased array beamforming image for 55 percent motor speed, left rear top rotor, 4585 Hz.

Figure 17.—Partitions for source separation, red box for advancing blade, green box for hub/motor region, blue box for retreating blade. Phased array beamforming image for 55 percent motor speed, left rear top rotor, 4585 Hz.

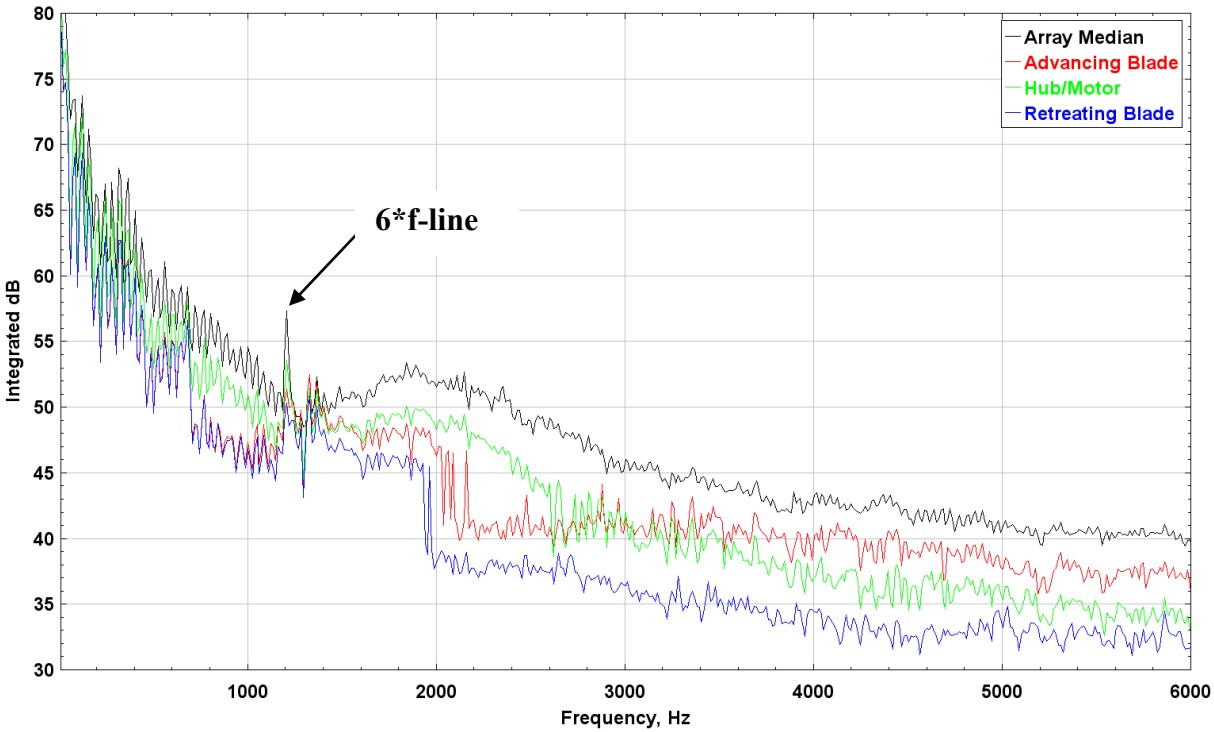

Figure 18.—Phased array spectra with partitions for 55 percent motor speed, left rear top rotor.

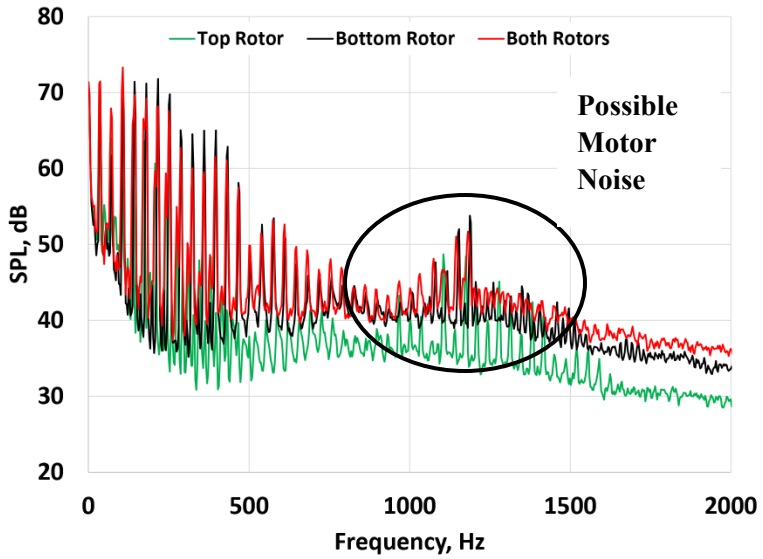

Figure 19.—SPL for left front top, left front bottom and left front both rotors, 45 percent speed, 0 degrees, microphone 3.

The protrusion of motor tones above the propeller noise is evident as the propeller noise is reduced. Figure 19 shows comparisons of the spectra for the left front rotor, left bottom rotor and both rotors operating at 45 percent speed at a distance of 100 ft (microphone 3), and directly ahead of the vehicle (0 degrees). When only the top rotor is operating, the rotor noise is reduced and the motor tones are more pronounced. This suggests that UAM vehicles with only top-mounted rotors could have higher contributions from the motors on the overall sound level.

The overall sound pressure levels (OASPL) have been computed from the narrowband spectra by summing the SPL as described in Appendix C, and all results shown in Figure 58 to Figure 60. Results for 35, 45, and 55 percent motor speeds are shown in Figure 20 through Figure 22 for the line of microphones at 0 degrees. Shown are OASPL versus distance to each microphone on a log scale for various combinations of rotors. The acoustic far field can be identified when the falloff of OASPL reaches 6 dB per doubling of distance. For convenience, a line has been added for this criterion and shows that the far field is reached by about 100 ft for most configurations.

The plots confirm that there is insufficient margin from the ambient noise levels for microphones located 200 ft away and the vehicle operating at lower speeds. This will likely improve for higher power settings required for hover and flyover tests.

The data from the various combinations of rotors reveal that the bottom rotor is louder than the top rotor by about 5 to 10 dB. This is expected since the bottom rotor operates in the wake of the top rotor and the support arm. In fact, the noise levels from the bottom rotor are similar to levels observed when both rotors are operating as a contra-rotating pair. Similar trends have been observed with contra-rotating propellers for axial thrust. Reducing the diameter of the bottom rotor to avoid interactions with the tip vortices and varying the number of blades should be considered for noise reduction based on lessons learned from propellers (Ref. 6). Note that no attempt has been made to correct the sound levels for equal thrust.

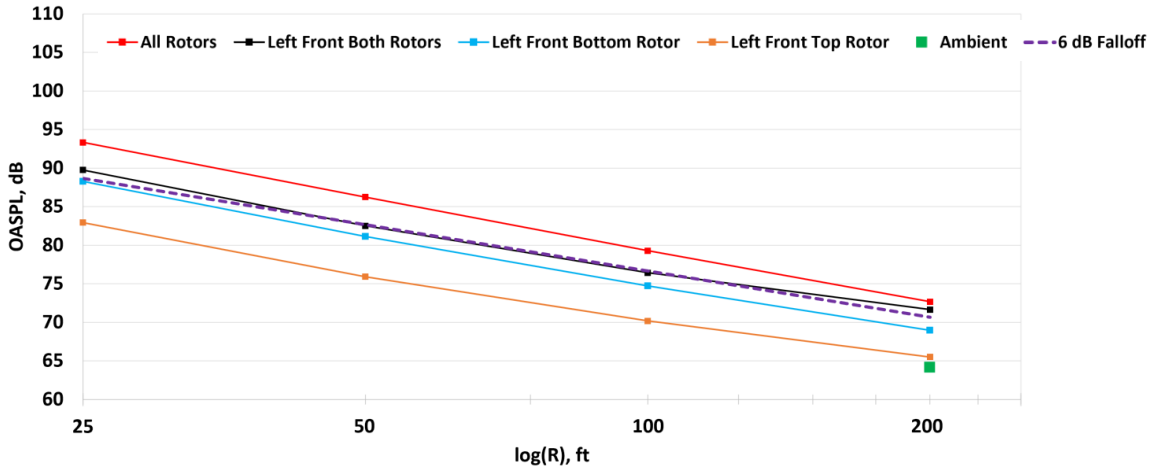

Figure 20.—OASPL versus microphone distance, 0 degrees, 35 percent motor speed.

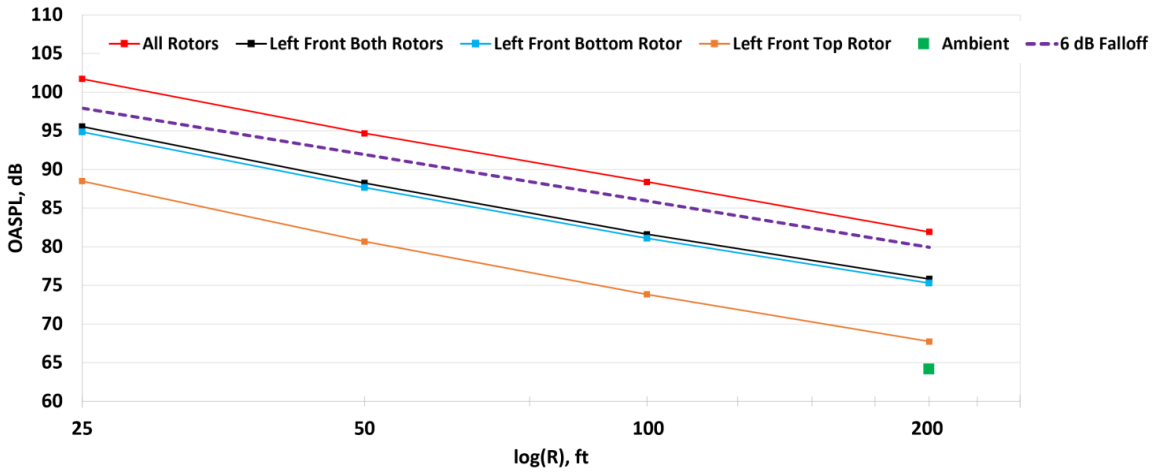

Figure 21.—OASPL versus microphone distance, 0 degrees, 45 percent motor speed.

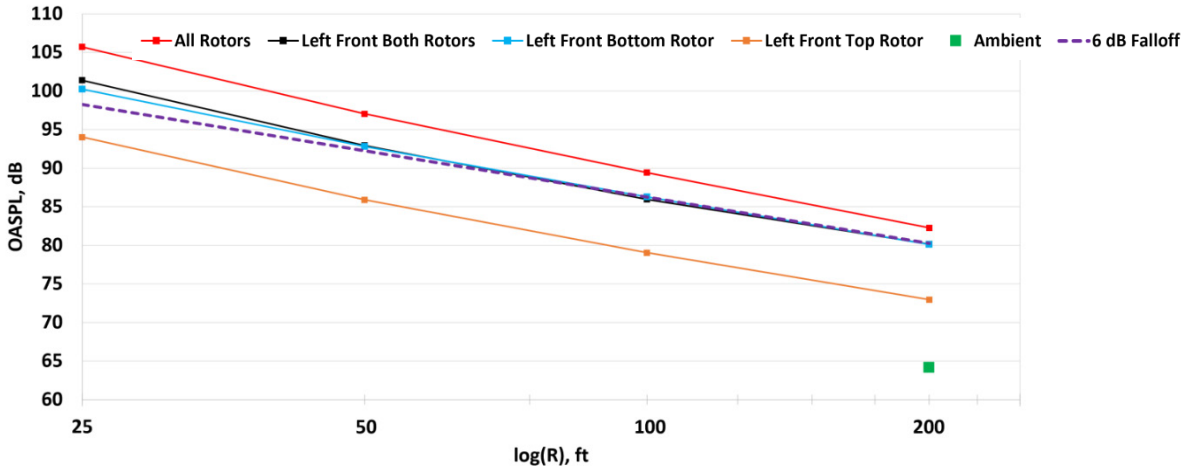

Figure 22.—OASPL versus microphone distance, 0 degrees, 55 percent motor speed.

The measured acoustic spectra have high sound levels at low frequencies (<50 Hz). The frequency range of the microphones used in the test extends down to 3.15 Hz. The selection of the lower bound of frequencies included in the integration for OASPL has a significant impact on the level. The International Civil Aviation Organization (ICAO) standards (Ref. 7) requires integration across the 1/3-octave bands centered on 50 Hz through 10 kHz. This means the integration of narrowband data is done between 44.7 and 11,220 Hz including the lower and upper band limits. If frequencies below 44.7 Hz are important for annoyance evaluations of UAM vehicles, the standard 1/3-octave bands used by ICAO may need to be extended to lower frequency bands. Additionally, low frequency noise can couple with vehicle/building structures and even human body resonances that require different metrics for annoyance.

Table 5 shows how the OASPL values vary depending on which frequency range is used. The OASPL levels can vary by 10 to 15 dB for the selected case of the left front top rotor operating at 45 percent speed. A-weighted OASPL values are also included. Applying the A-weight filter eliminates the sensitivity to the low frequency levels.

Figure 23 through Figure 25 show the A-weighted sound levels for 35, 45, and 55 percent motor speeds for selected test cases. Plots of OASPL versus microphone distance for all test conditions are included in Appendix C. Both the unweighted and A-weighted sound levels are included. All of the plots use a frequency range of 44.7 to 11,220 Hz for the OASPL calculations.

TABLE 5.—OASPL LEVELS AT FOUR MICROPHONE LOCATIONS, 45 PERCENT MOTOR SPEED, LEFT FRONT TOP ROTOR, 0 DEGREES

Microphone, (distance)	OASPL, (dB)		A-weighted OASPL, (dBA)	
	All Bands[a]	ICAO Bands[b]	All Bands	ICAO Bands
1 (25’)	103.8	88.5	82.2	82.2
2 (50’)	86.3	80.7	73.3	73.3
3 (100’)	77.4	73.8	65.2	65.2
4 (200’)	71.4	67.7	57.8	57.8

[a]All Bands: 3.15 to 11,220 Hz
[b]ICAO Bands: 44.7 to 11,220 Hz

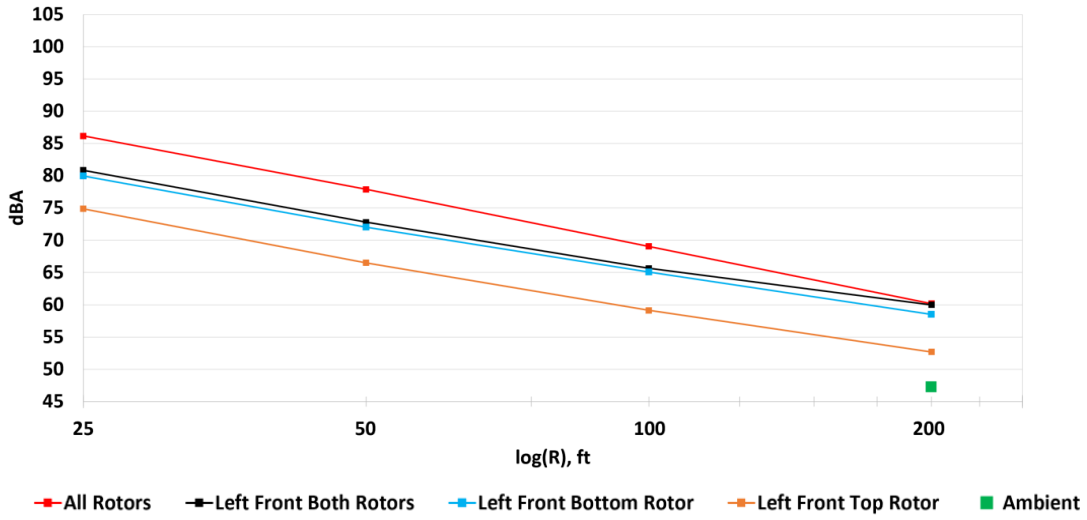

Figure 23.—A-weighted OASPL versus microphone distance, 0 degrees, 35 percent motor speed.

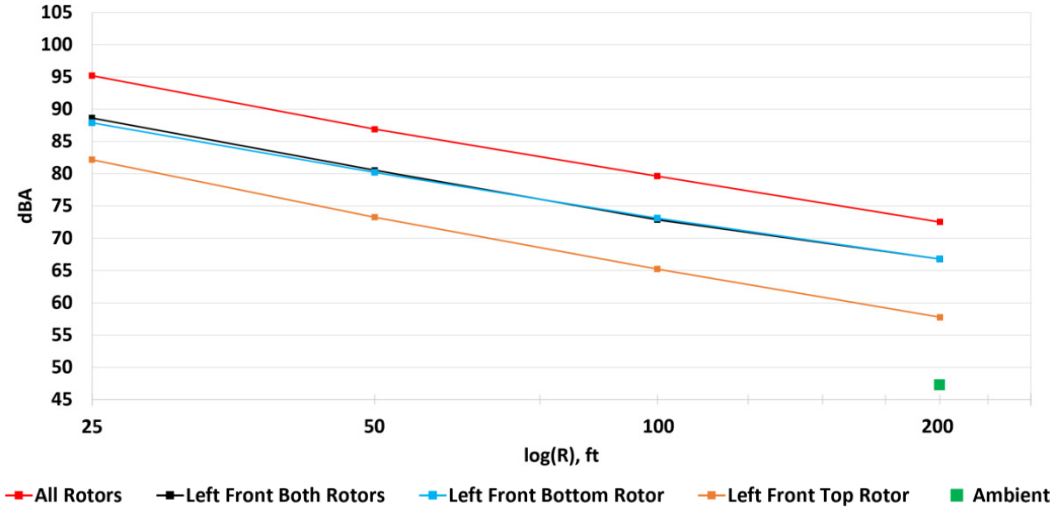

Figure 24.—A-weighted OASPL versus microphone distance, 0 degrees, 45 percent motor speed.

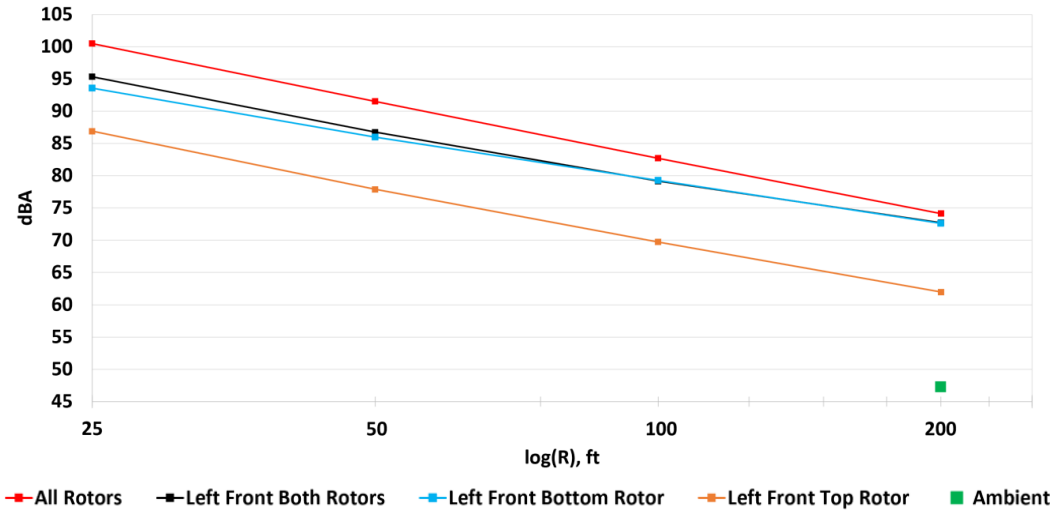

Figure 25.—A-weighted OASPL versus microphone distance, 0 degrees, 55 percent motor speed.

Figure 26.—Test team from left to right: Thaddeus Bort, Jr., Andrew Schaub, Justin Jantzen, Zach Carlton, Brenda Henderson, Dennis Huff, Jordan Cluts, Ed Kurdi, Jeffrey Bennett, John Graber (not pictured); November 6, 2019.

A group picture of the test team is shown in Figure 26. The team consisted of people from the NASA Glenn Research Center and Moog, Inc.

Conclusions

Ground tests of Moog's SureFly all-electric research vehicle have provided an initial assessment of noise characteristics from a UAM-class aircraft. The tests were conducted to help guide future work that will include hover and flyover noise measurements. The acoustic far field was measured to begin 100 ft from the test vehicle for motor speeds up to 55 percent (just below liftoff). Observations during the test included modulation sounds for several test conditions that were shown to be possible from multiple rotors operating at slightly different rotational speeds. Narrowband acoustic data and phased microphone array data show propeller tones and broadband noise, and evidence of motor noise near computed harmonics of the electrical line frequencies. Ambient noise levels were close enough to the measured spectra for lower speeds to be a concern as the distance away from the vehicle reached 200 ft. A quieter location for future noise measurements is desirable.

Tests included running various combinations of the eight propellers, including just the top and/or bottom propeller from a single support arm. Results show that the noise from the bottom propellers is about 5 to 10 dB louder than the top propellers. This indicates that the interaction of the top propeller wake and support arm wake with the lower rotor is an important noise source. Noise from the motors could become more important for UAM vehicles with only top-mounted propellers. Noise reduction techniques used for contra-rotating axial thrust propellers should be investigated in future tests.

The presence of low frequency noise (<50 Hz) suggests that careful selection of annoyance metrics might be necessary particularly for near-field considerations around vertiports for example. ICAO guidelines for flyover noise evaluations neglect the low frequencies, as does applying an A-weight filter. It is possible that the low frequency noise could couple with nearby building structures or contribute to vehicle interior noise.

Appendix A.—Rotor Speed Data

The speeds for each motor on the SureFly vehicle were recorded by Moog using a telemetry system. Files were provided in Excel format for each of the test conditions shown in Table 2. The data files are labeled as shown in Figure 27.

The motor speed data are plotted in Figure 28 to Figure 35 for each test condition. The percent speed conditions are labeled. The legend indicates which motor is powered with colors that correspond to the line plots. For cases where only one rotor is powered, the paired rotor windmills at a slower speed as indicated.

A_all-rotors-first-set.csv	2/8/2021 1:23 PM	Microsoft Excel Com...	1,046 KB
B_left-front-top-rotor.csv	2/8/2021 1:23 PM	Microsoft Excel Com...	1,033 KB
C_left-front-bottom-rotor.csv	2/8/2021 1:23 PM	Microsoft Excel Com...	1,101 KB
D_left-front-both-rotors.csv	2/8/2021 1:23 PM	Microsoft Excel Com...	935 KB
E_left-rear-top-rotor.csv	2/8/2021 1:23 PM	Microsoft Excel Com...	890 KB
F_left-rear-bottom-rotor.csv	2/8/2021 1:49 PM	Microsoft Excel Com...	553 KB
G_left-rear-both-rotors.csv	2/8/2021 1:23 PM	Microsoft Excel Com...	496 KB
H_all-rotors-second-set.csv	2/8/2021 1:23 PM	Microsoft Excel Com...	881 KB

Figure 27.—Motor rpm data files.

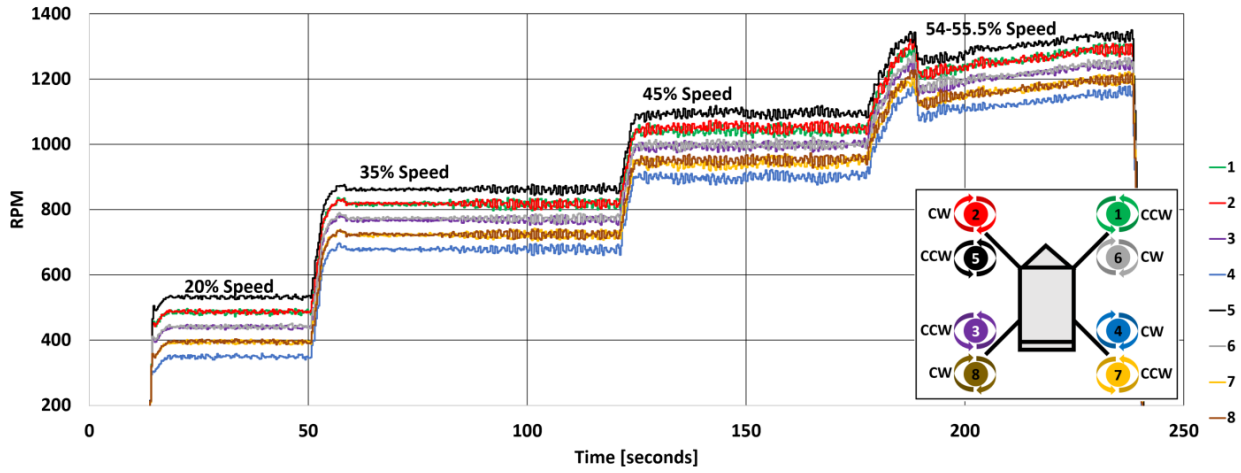

Figure 28.—All rotors (1-8), first run.

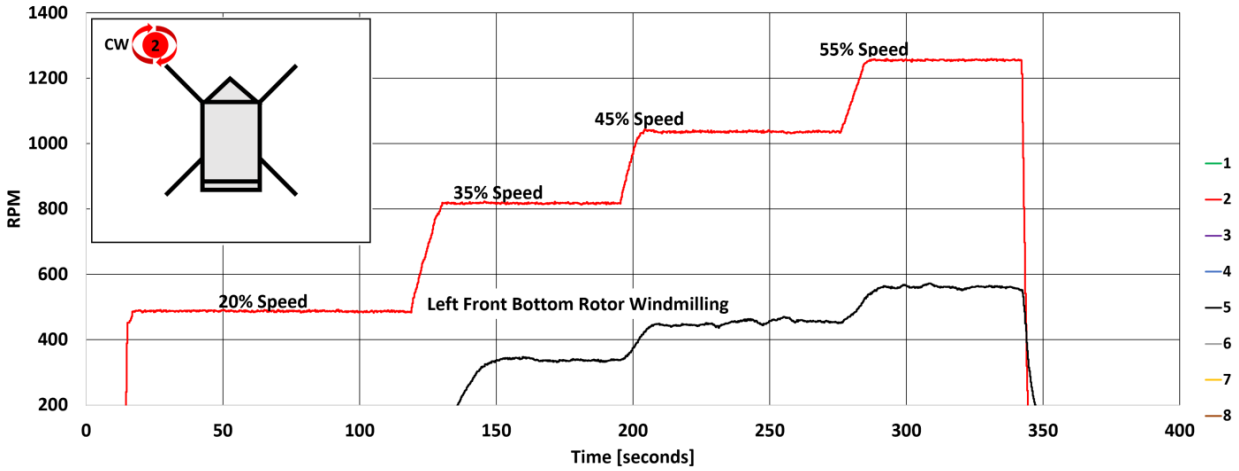

Figure 29.—Left front top rotor (2).

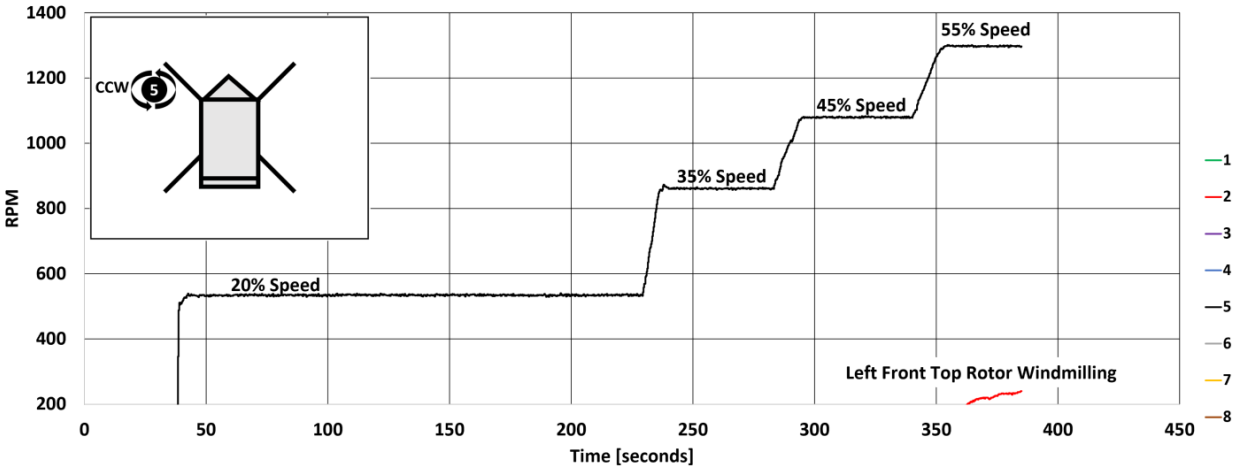

Figure 30.—Left front bottom rotor (5).

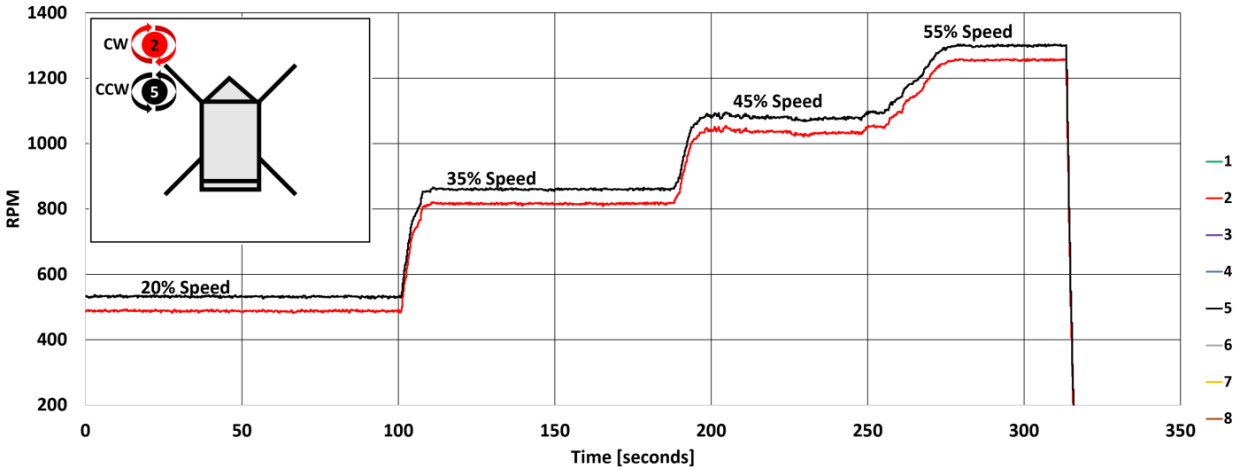

Figure 31.—Left front both rotors (2 and 5).

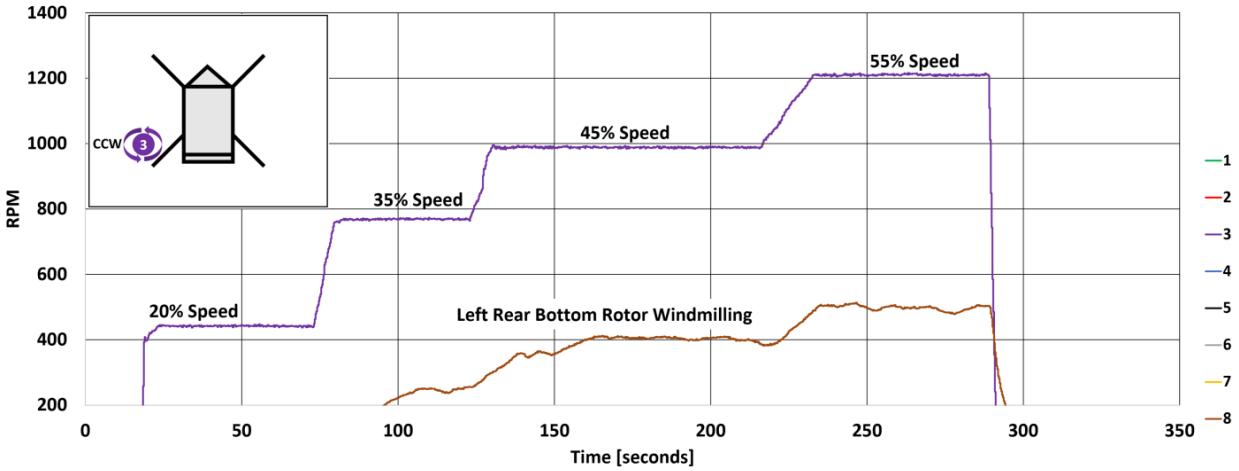

Figure 32.—Left rear top rotor (3).

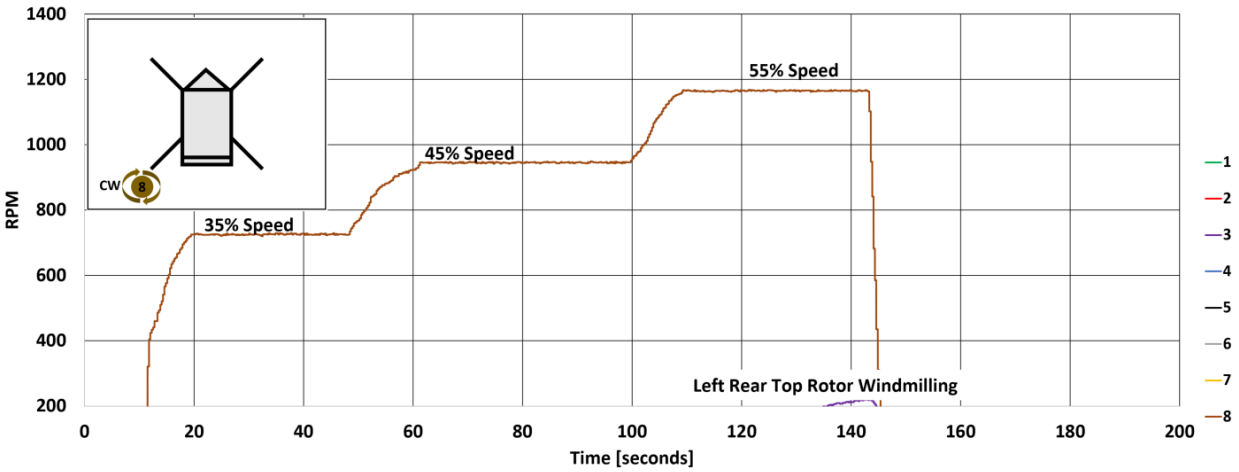

Figure 33.—Left rear bottom rotor (8).

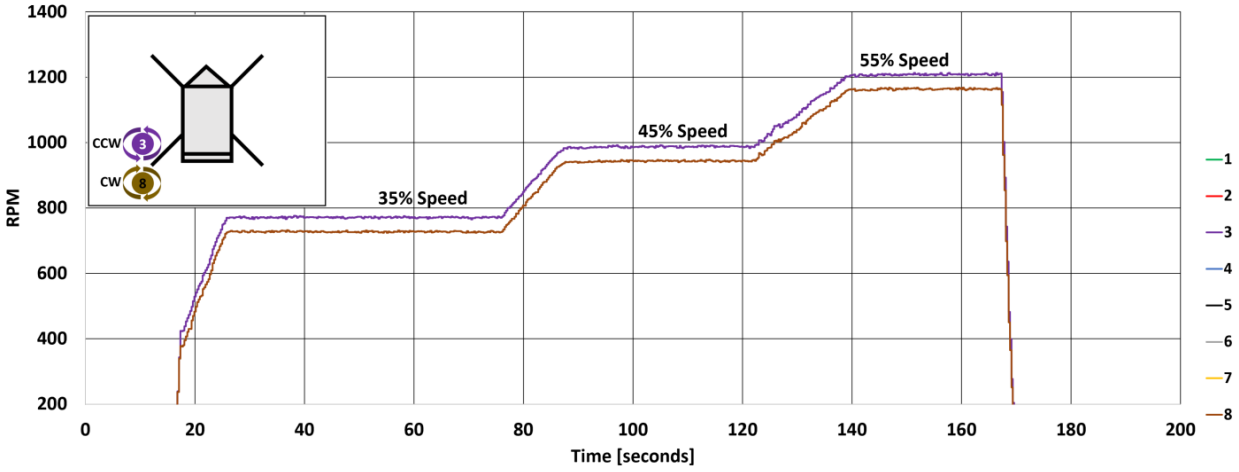

Figure 34.—Left rear both rotors (3 and 8).

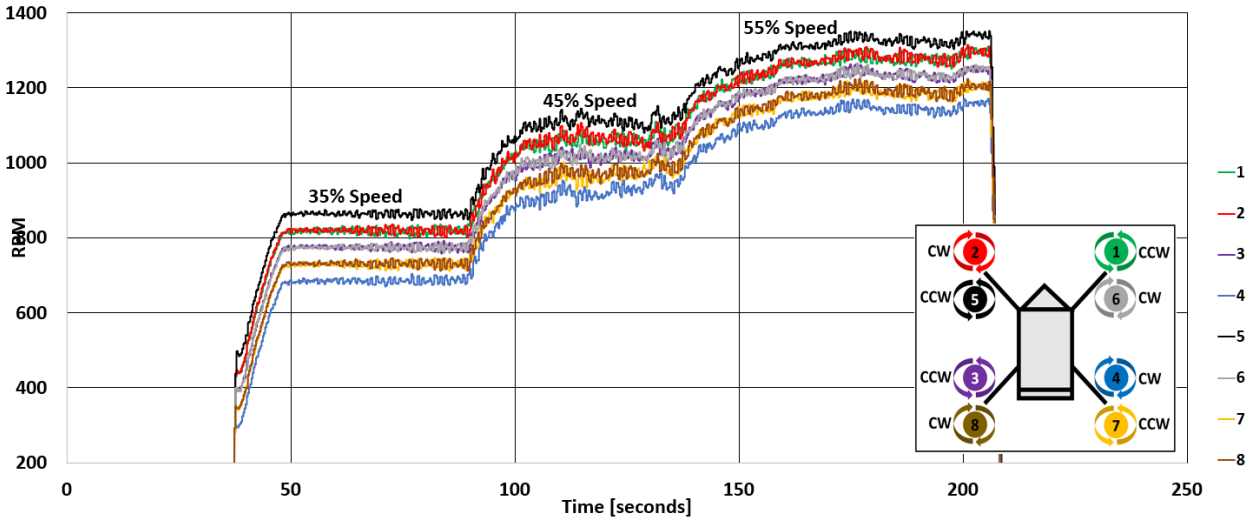

Figure 35.—All rotors (1-8) second run.

Appendix B.—Acoustic Data

The sound pressure time histories were stored for each microphone and processed to narrowband sound pressure level (SPL) and overall sound pressure level (OASPL). The sample rate was 50000 Hz and the data acquisition time was 20 s. With an FFT size of 16384, the bandwidth is 3.0518 Hz. The acoustic data have been plotted using Microsoft Excel for each test condition listed in Table 2 (Figure 36).

The narrowband SPL acoustic data are plotted for each test condition and speed, for the two radial arrays of microphones (0 and –45 degrees) shown in Figure 3. Two ranges of frequencies are shown for clarity. The first set of data with all rotors operating (A) was not used due to the speed variations around 55 percent speed (Figure 28). The ambient noise levels are also plotted for the outer microphone in each line (i.e., #4 and #8) for runs 0008 and 0045.

Figure 36.—Acoustic data files (processed).

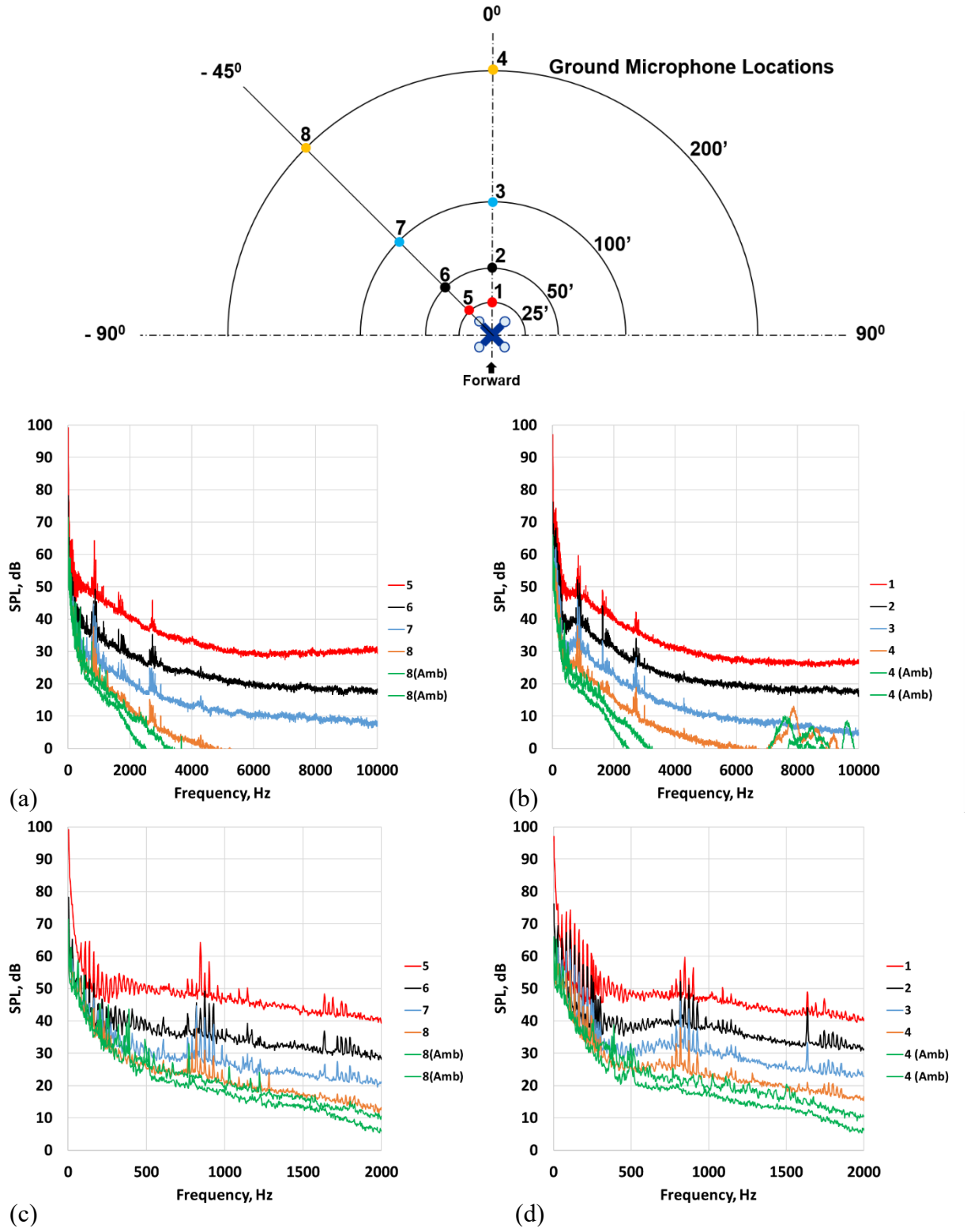

Figure 37.—SPL for left front top rotor, 35 percent speed, run number 0011. (a) –45 degrees, 0 to 10 kHz. (b) 0 degrees, 0 to 10 kHz. (c) –45 degrees, 0 to 2 kHz. (d) 0 degrees, 0 to 2 kHz.

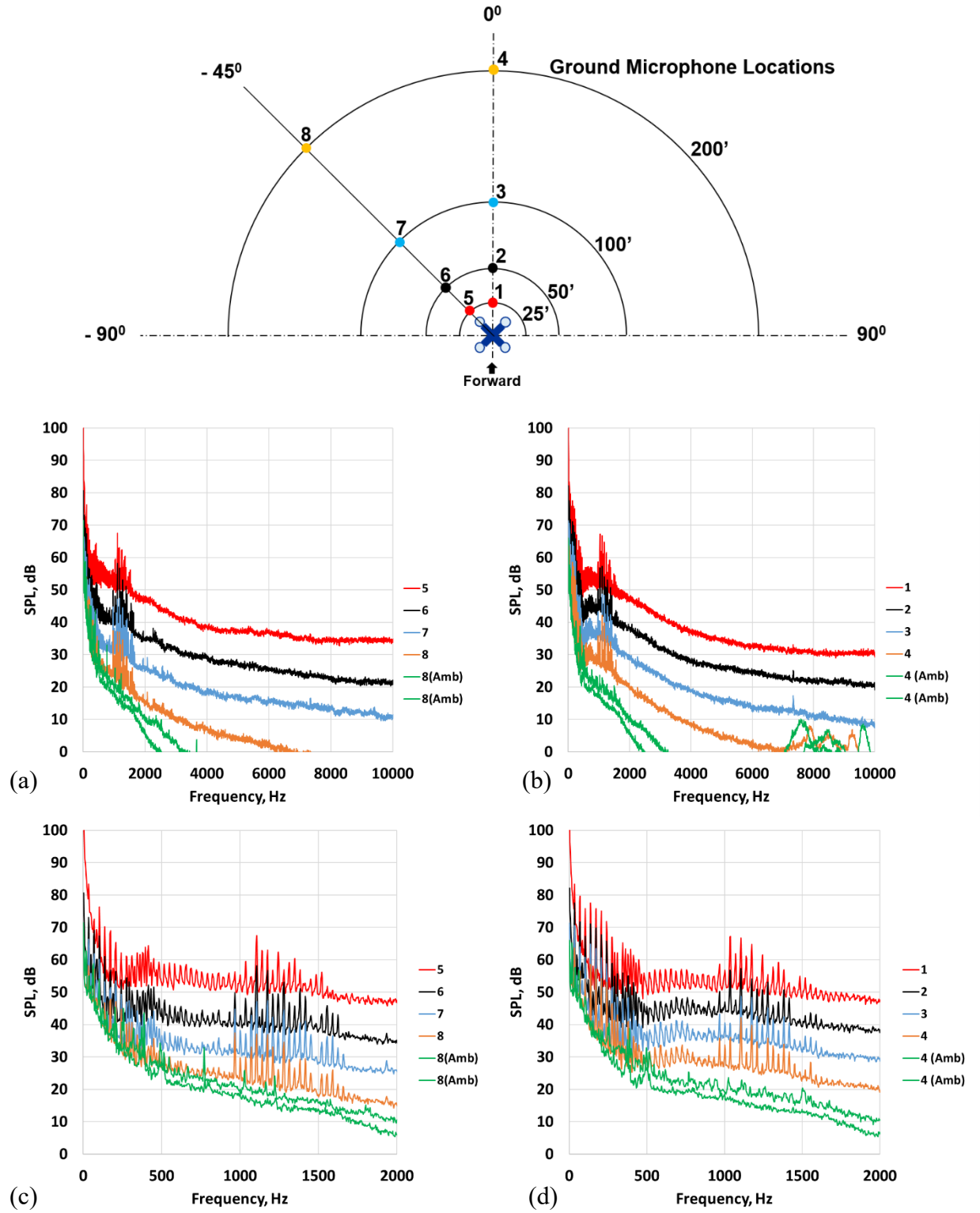

Figure 38.—SPL for left front top rotor, 45 percent speed, run number 0013. (a) –45 degrees, 0 to 10 kHz. (b) 0 degrees, 0 to 10 kHz. (c) –45 degrees, 0 to 2 kHz. (d) 0 degrees, 0 to 2 kHz.

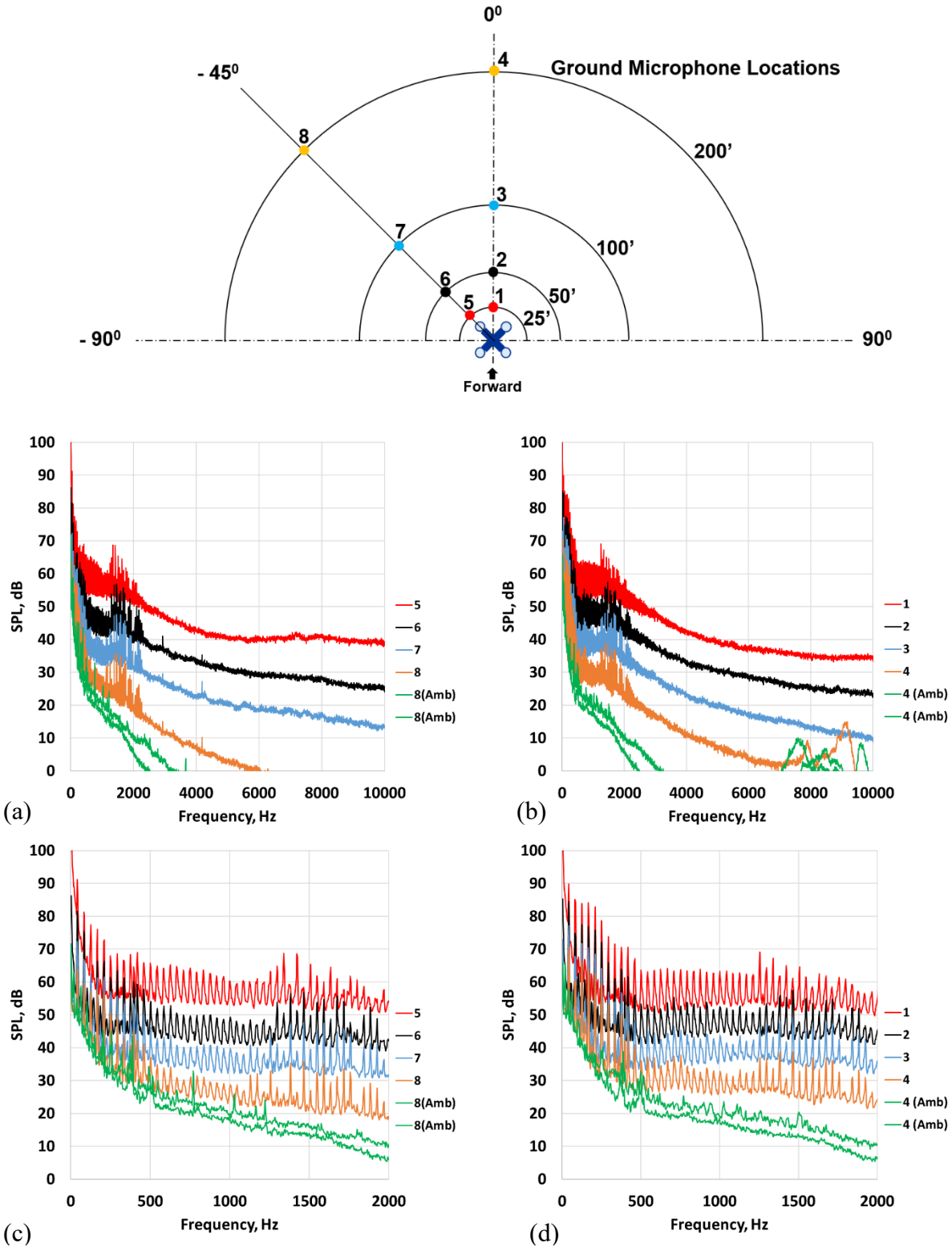

Figure 39.—SPL for left front top rotor, 55 percent speed, run number 0014. (a) –45 degrees, 0 to 10 kHz. (b) 0 degrees, 0 to 10 kHz. (c) –45 degrees, 0 to 2 kHz. (d) 0 degrees, 0 to 2 kHz.

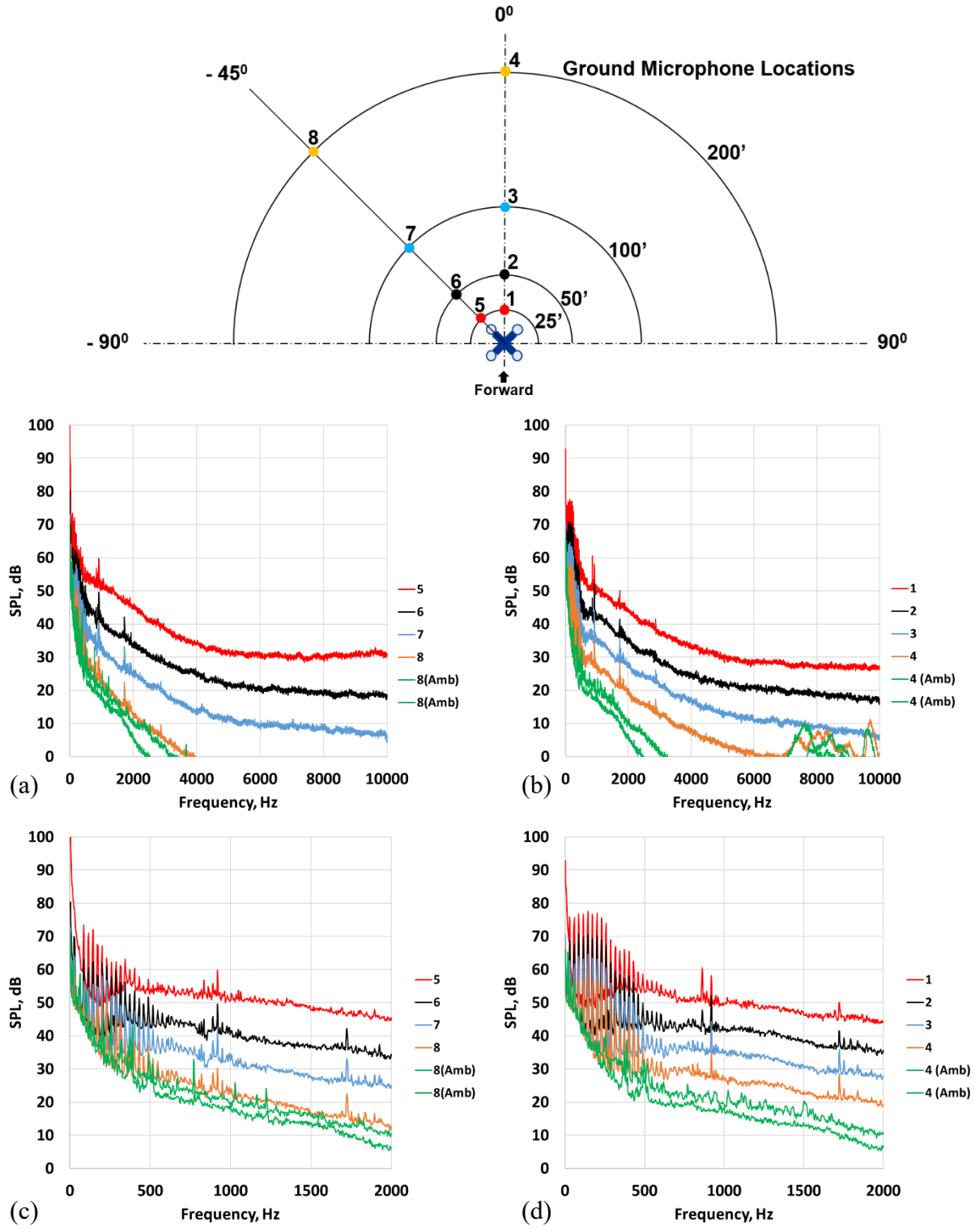

Figure 40.—SPL for left front bottom rotor, 35 percent speed, run number 0018. (a) –45 degrees, 0 to 10 kHz. (b) 0 degrees, 0 to 10 kHz. (c) –45 degrees, 0 to 2 kHz. (d) 0 degrees, 0 to 2 kHz.

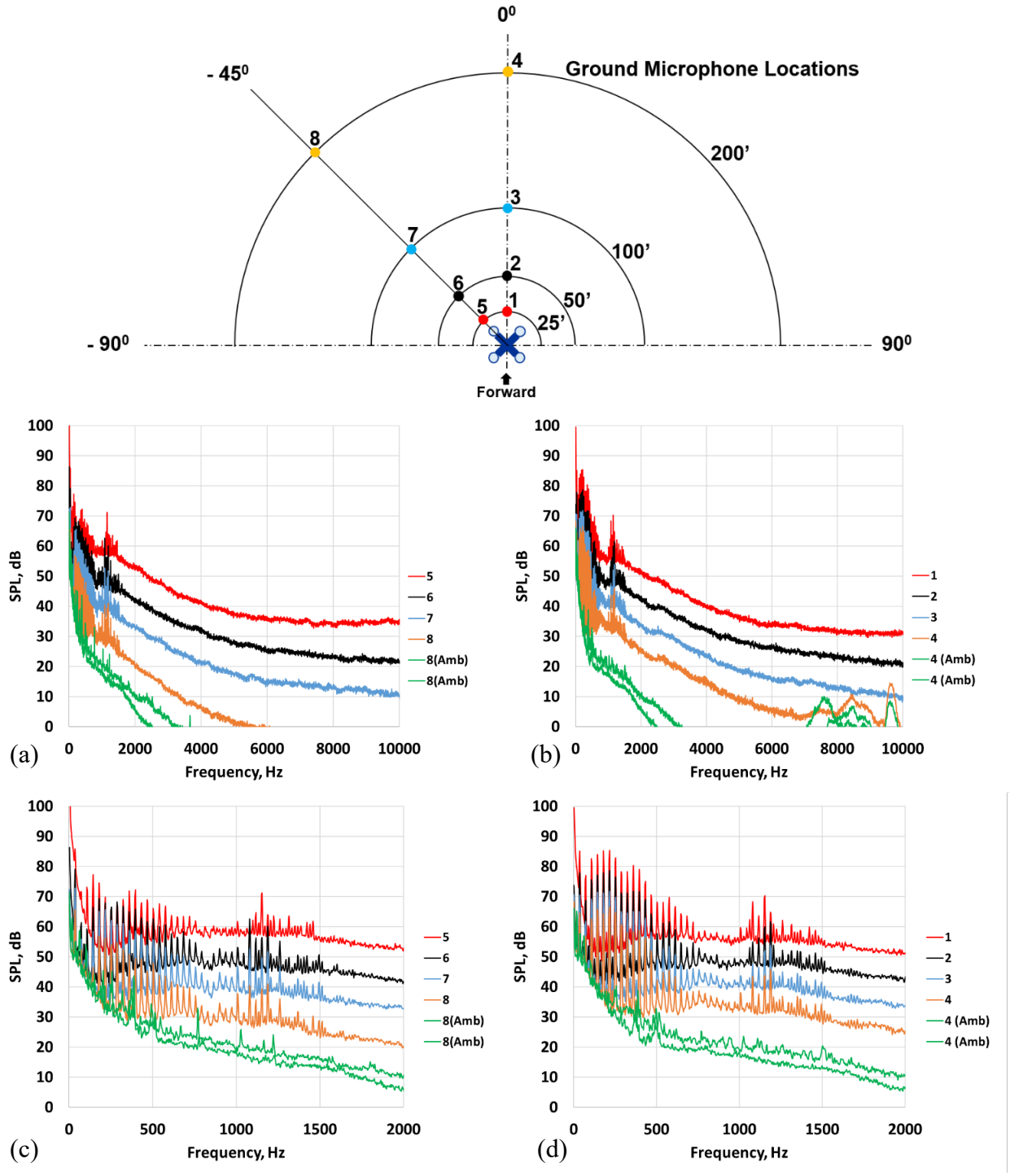

Figure 41.—SPL for left front bottom rotor, 45 percent speed, run number 0019. (a) –45 degrees, 0 to 10 kHz. (b) 0 degrees, 0 to 10 kHz. (c) –45 degrees, 0 to 2 kHz. (d) 0 degrees, 0 to 2 kHz.

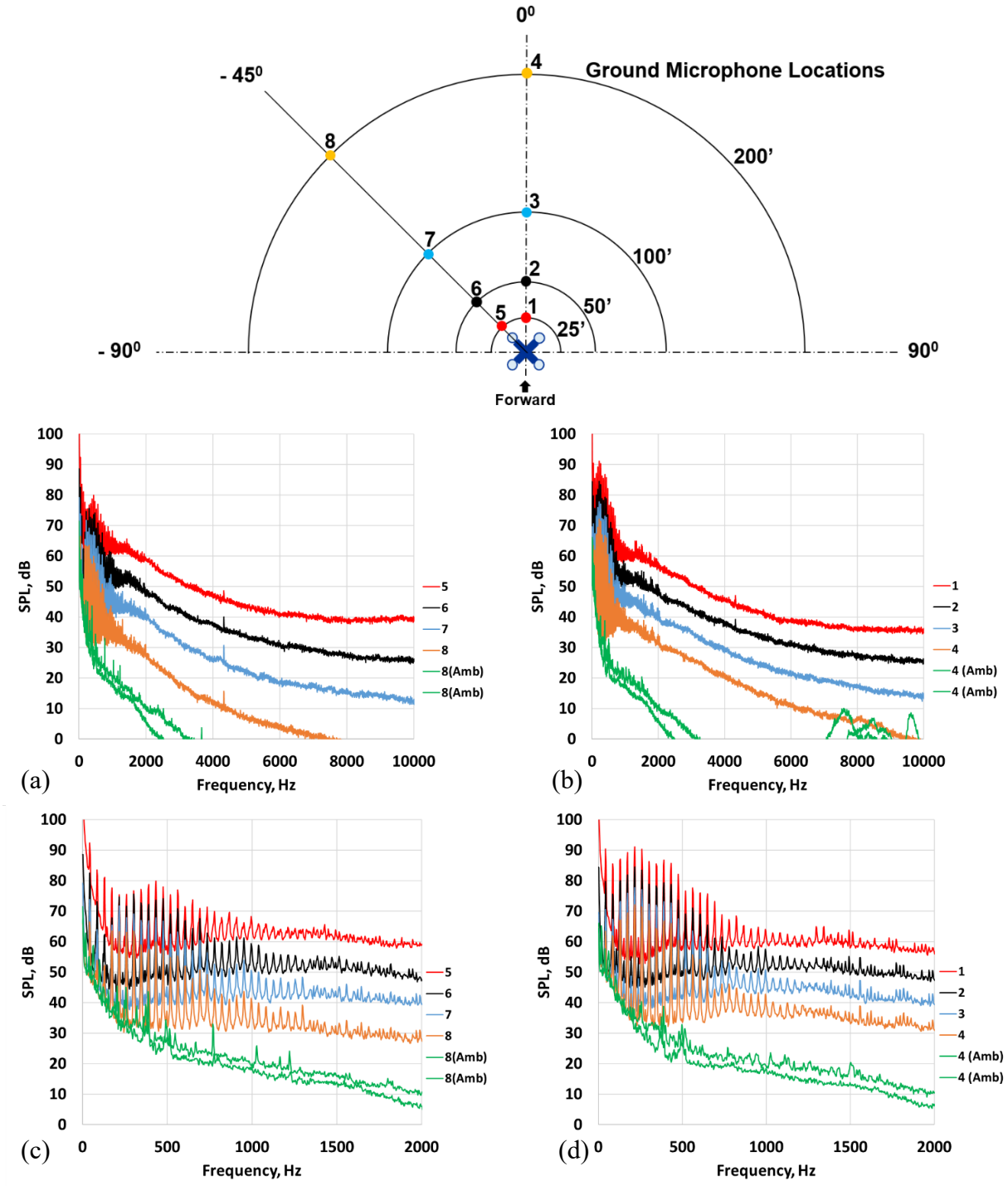

Figure 42.—SPL for left front bottom rotor, 55 percent speed, run number 0020. (a) –45 degrees, 0 to 10 kHz. (b) 0 degrees, 0 to 10 kHz. (c) –45 degrees, 0 to 2 kHz. (d) 0 degrees, 0 to 2 kHz.

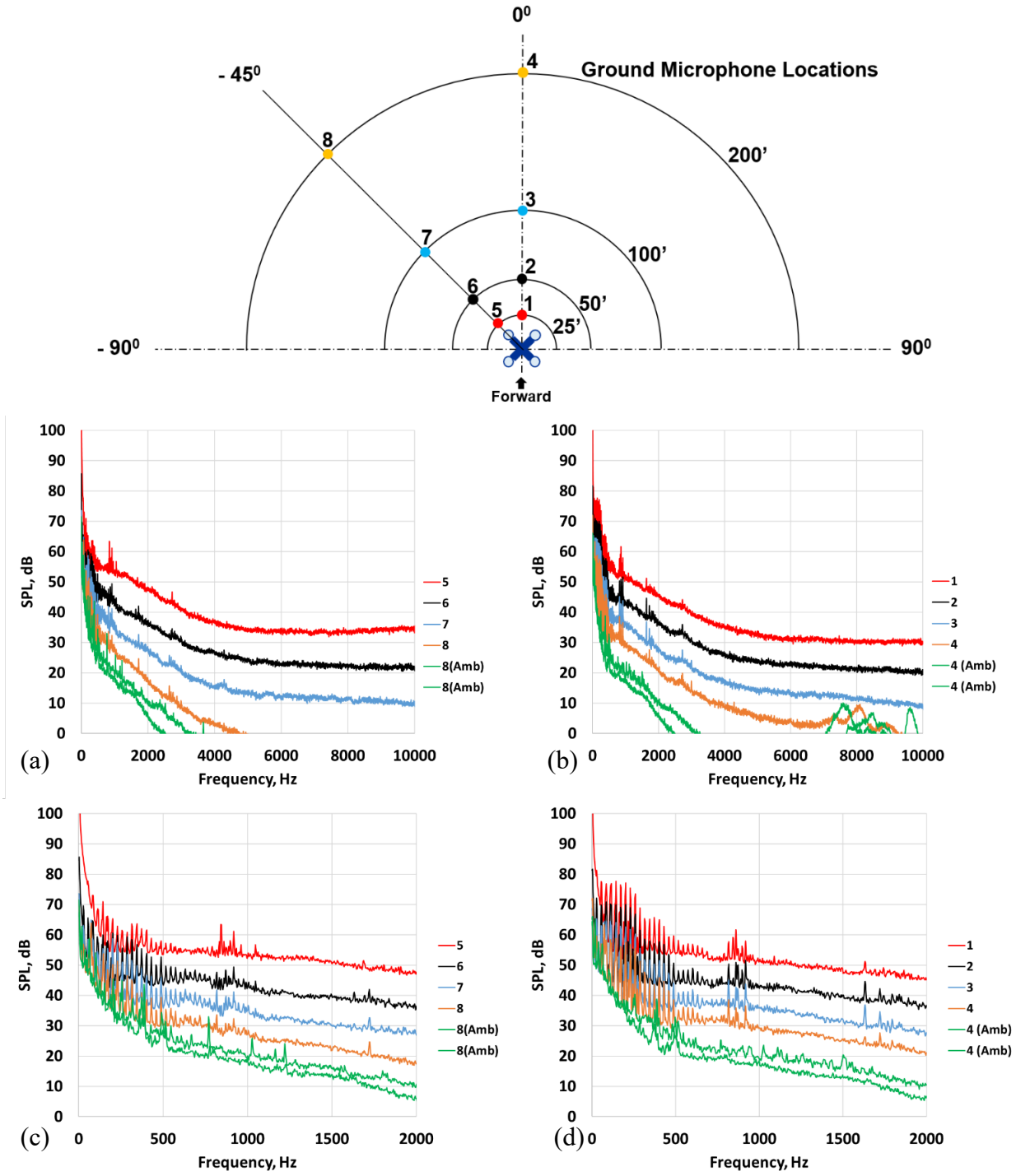

Figure 43.—SPL for left front both rotors, 35 percent speed, run number 0026. (a) –45 degrees, 0 to 10 kHz. (b) 0 degrees, 0 to 10 kHz. (c) –45 degrees, 0 to 2 kHz. (d) 0 degrees, 0 to 2 kHz.

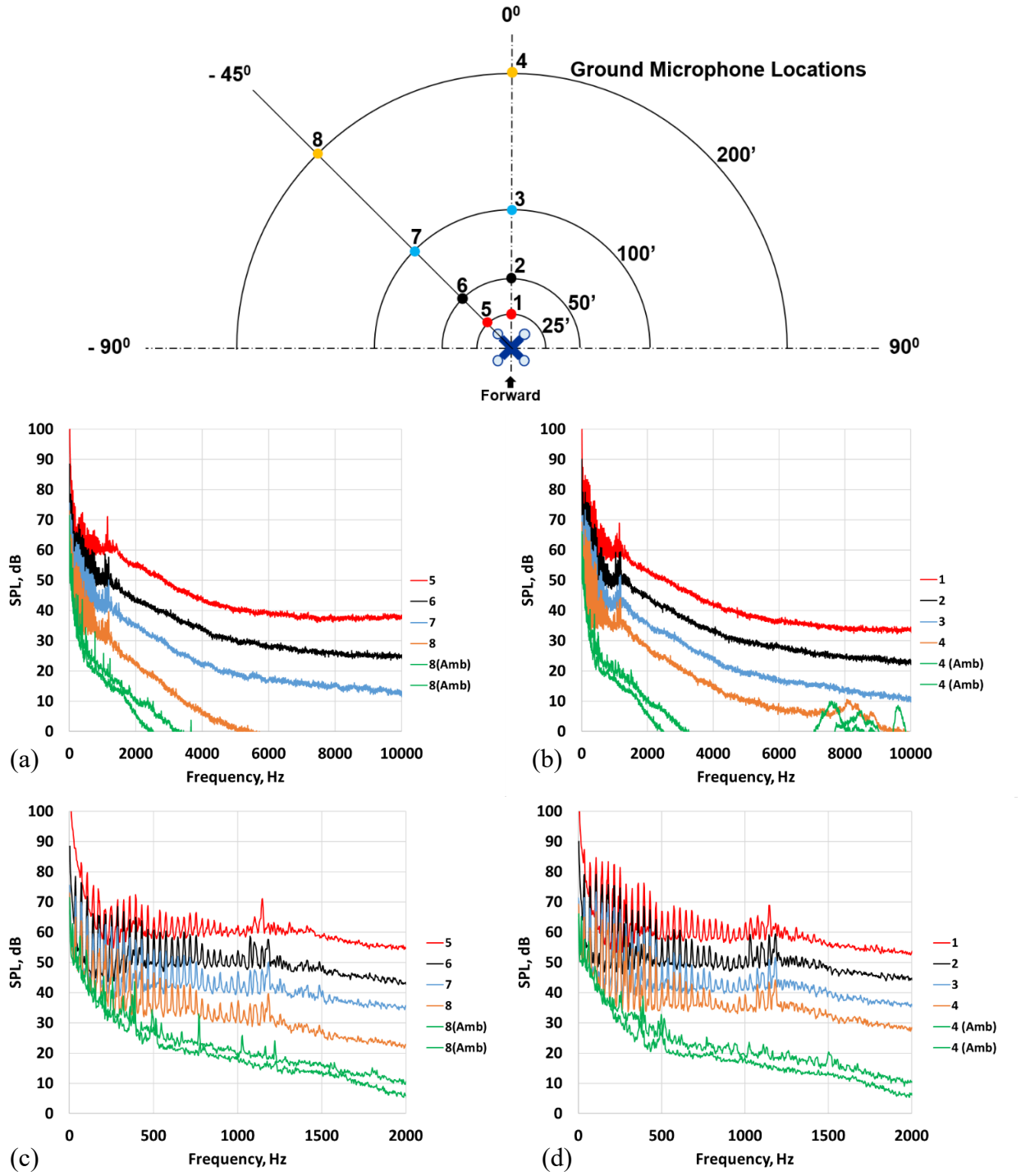

Figure 44.—SPL for left front both rotors, 45 percent speed, run number 0027. (a) –45 degrees, 0 to 10 kHz. (b) 0 degrees, 0 to 10 kHz. (c) –45 degrees, 0 to 2 kHz. (d) 0 degrees, 0 to 2 kHz.

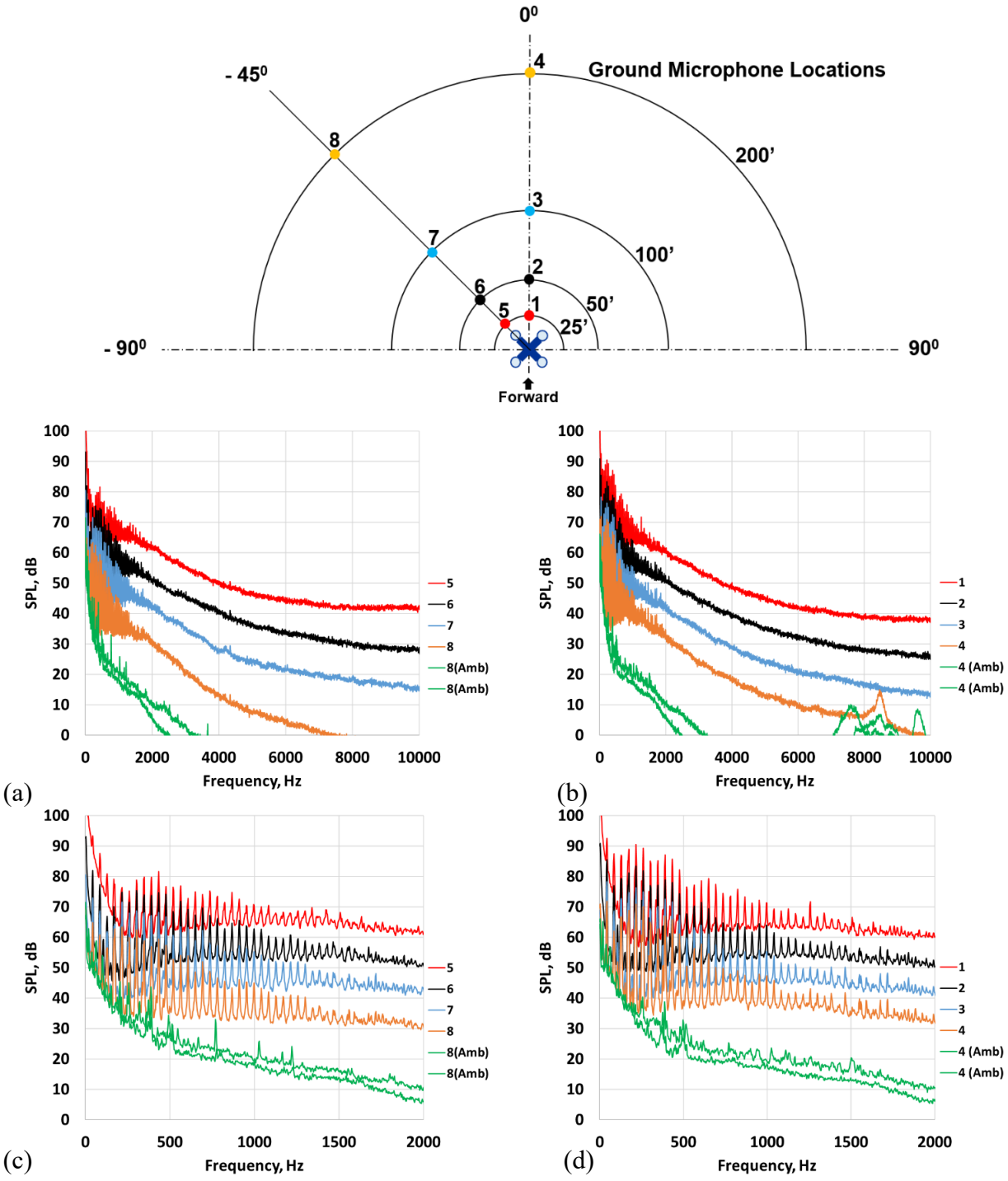

Figure 45.—SPL for left front both rotors, 55 percent speed, run number 0028. (a) –45 degrees, 0 to 10 kHz. (b) 0 degrees, 0 to 10 kHz. (c) –45 degrees, 0 to 2 kHz. (d) 0 degrees, 0 to 2 kHz.

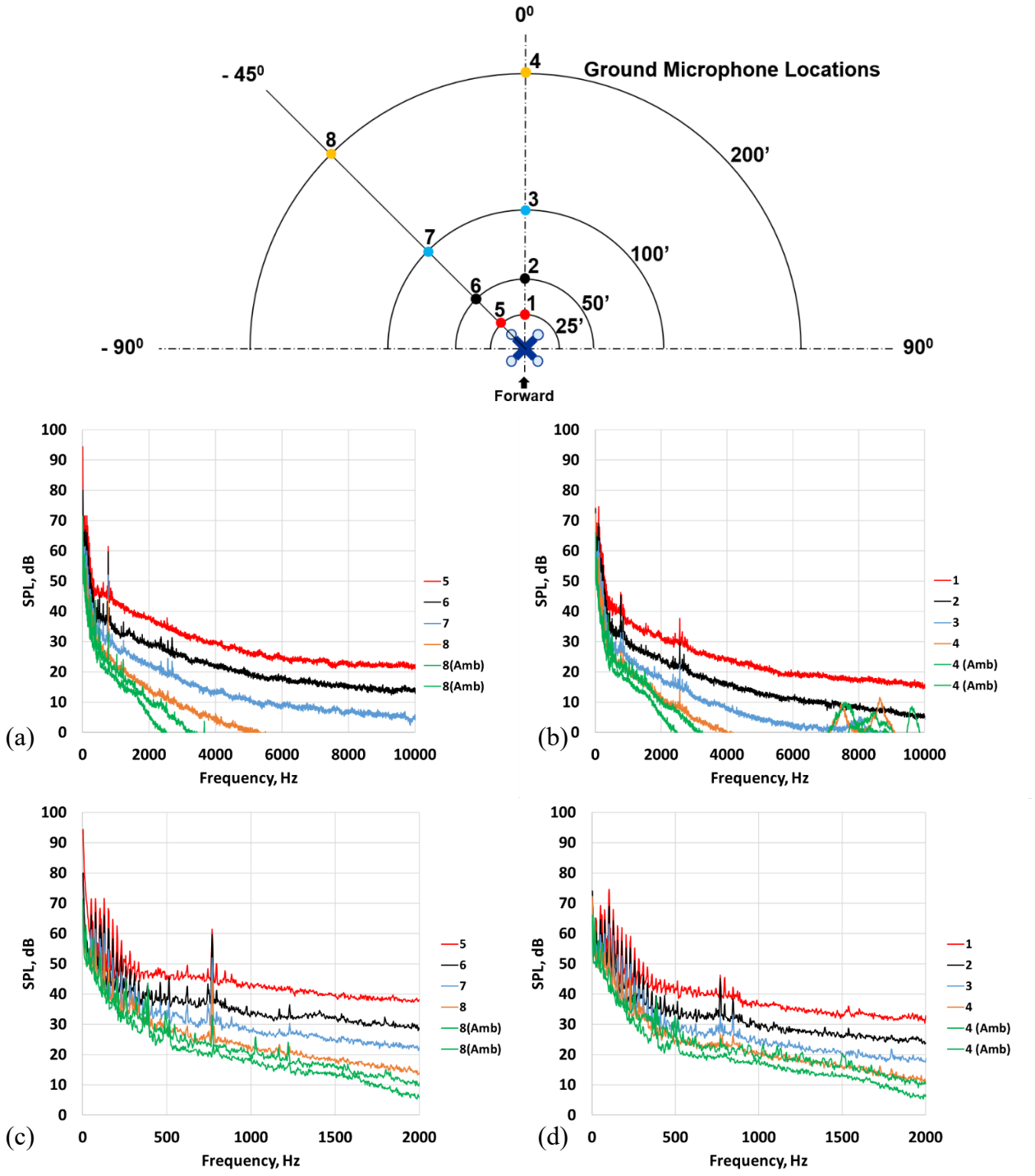

Figure 46.—SPL for left rear top rotor, 35 percent speed, run number 0030. (a) –45 degrees, 0 to 10 kHz. (b) 0 degrees, 0 to 10 kHz. (c) –45 degrees, 0 to 2 kHz. (d) 0 degrees, 0 to 2 kHz.

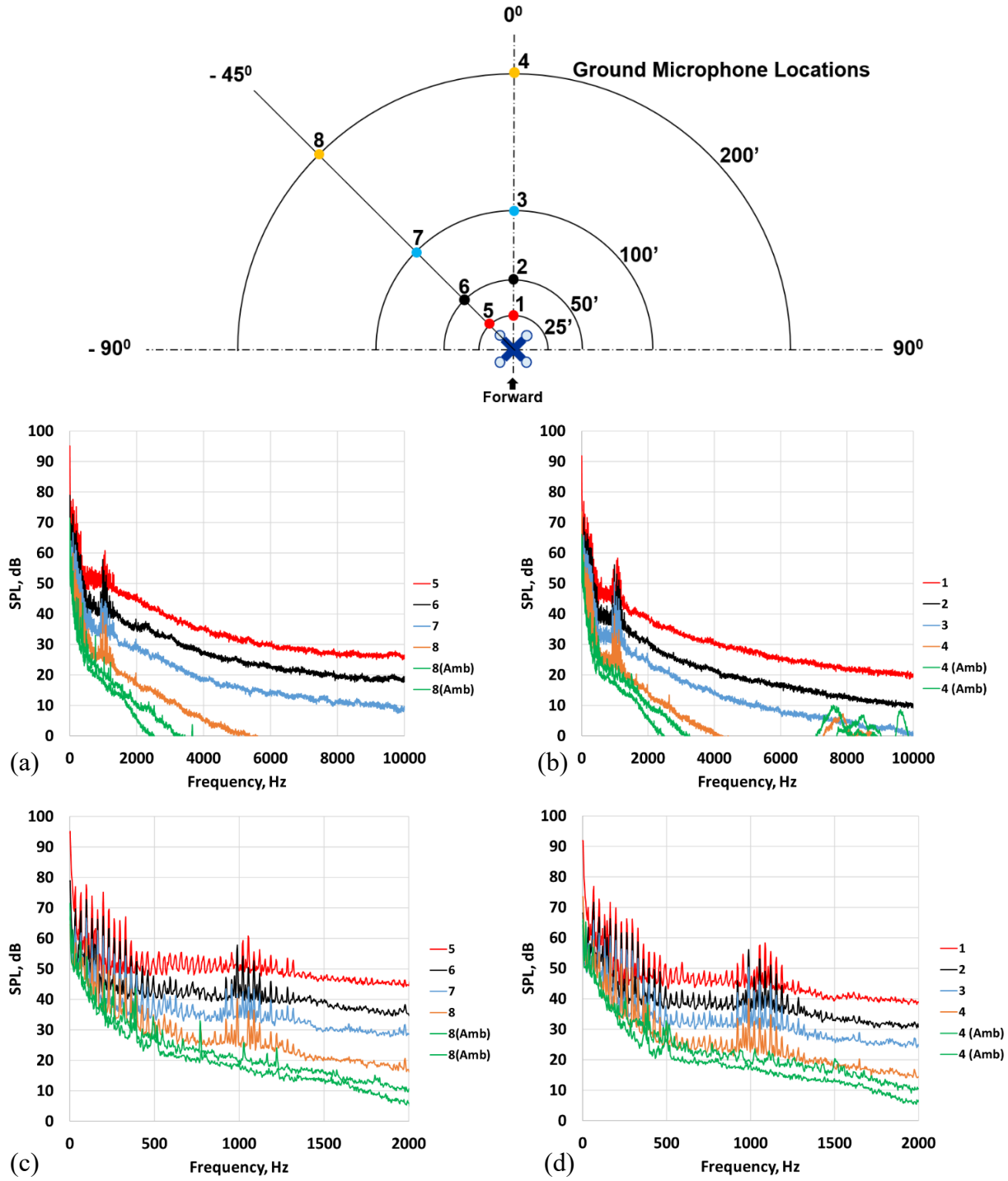

Figure 47.—SPL for left rear top rotor, 45 percent speed, run number 0032. (a) –45 degrees, 0 to 10 kHz. (b) 0 degrees, 0 to 10 kHz. (c) –45 degrees, 0 to 2 kHz. (d) 0 degrees, 0 to 2 kHz.

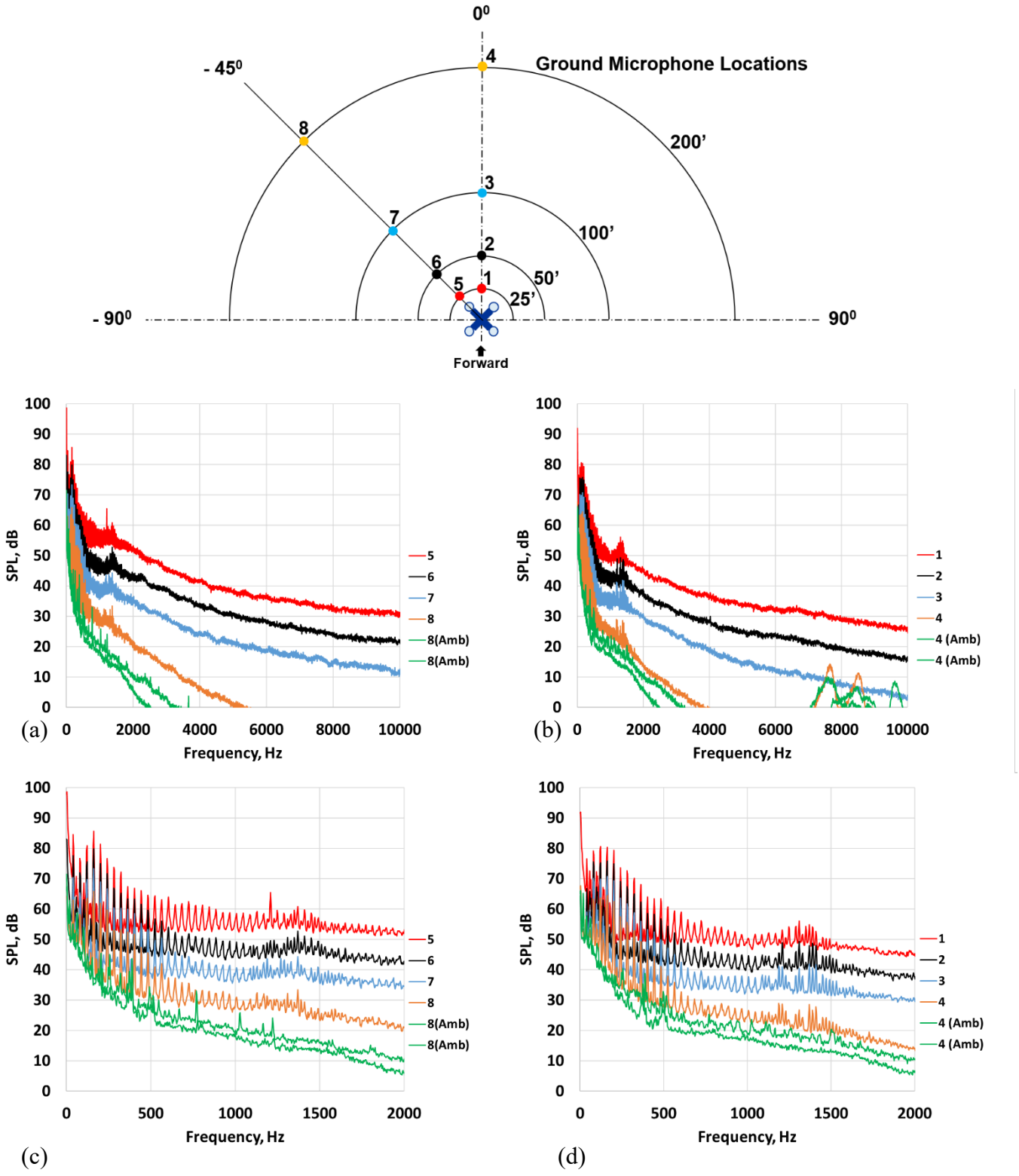

Figure 48.—SPL for left rear top rotor, 55 percent speed, run number 0033. (a) –45 degrees, 0 to 10 kHz. (b) 0 degrees, 0 to 10 kHz. (c) –45 degrees, 0 to 2 kHz. (d) 0 degrees, 0 to 2 kHz.

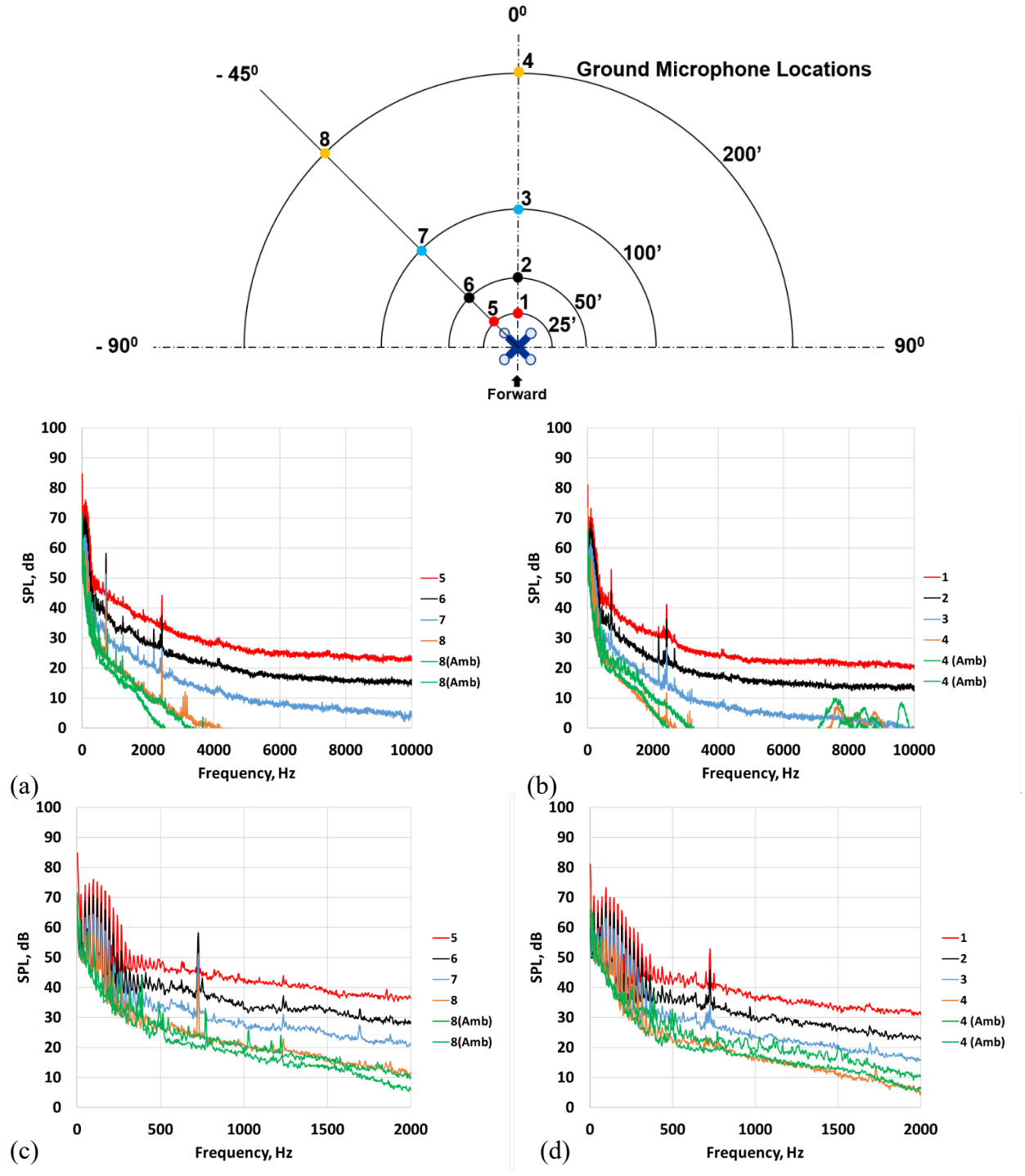

Figure 49.—SPL for left rear bottom rotor, 35 percent speed, run number 0035. (a) –45 degrees, 0 to 10 kHz. (b) 0 degrees, 0 to 10 kHz. (c) –45 degrees, 0 to 2 kHz. (d) 0 degrees, 0 to 2 kHz.

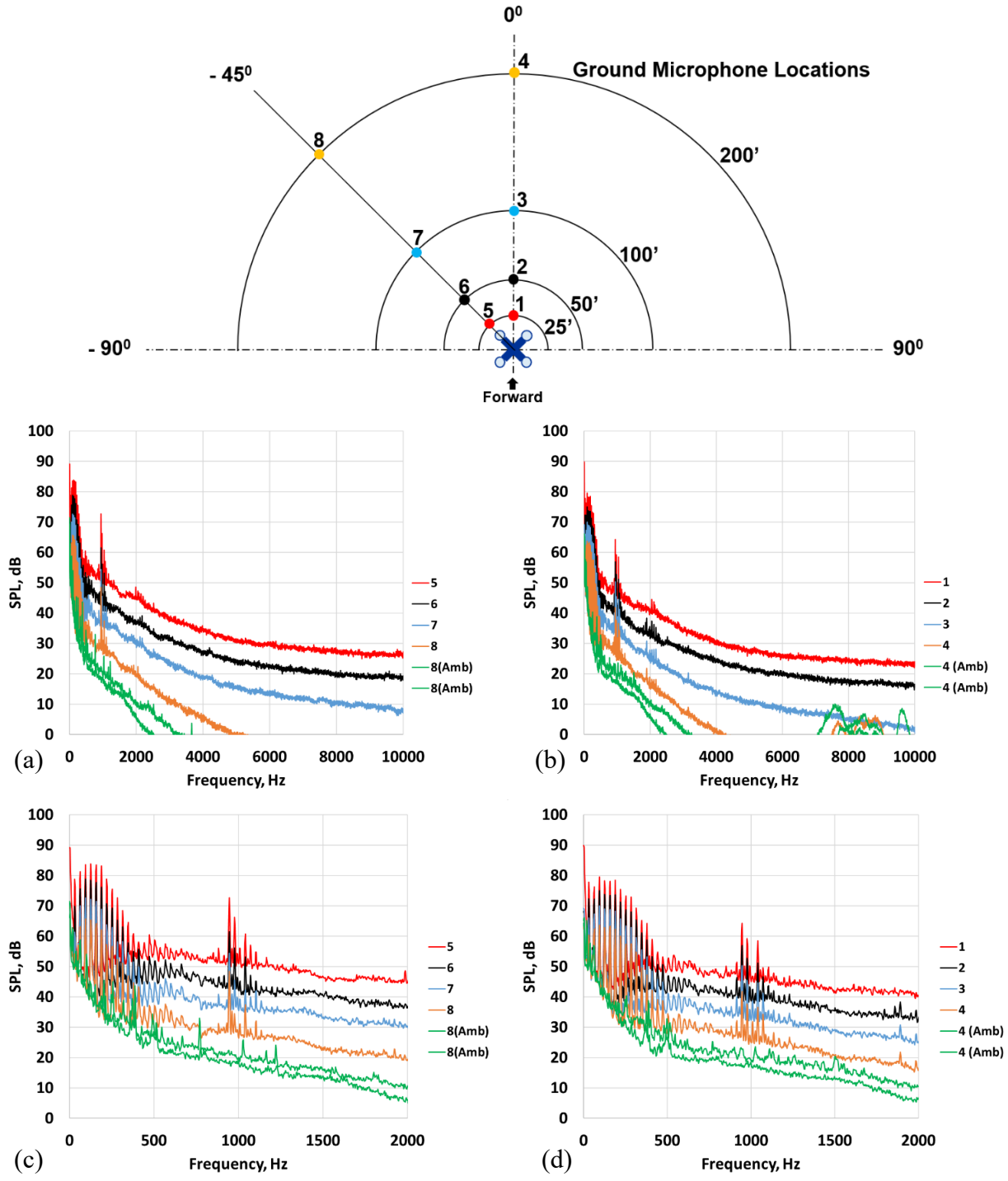

Figure 50.—SPL for left rear bottom rotor, 45 percent speed, run number 0036. (a) –45 degrees, 0 to 10 kHz. (b) 0 degrees, 0 to 10 kHz. (c) –45 degrees, 0 to 2 kHz. (d) 0 degrees, 0 to 2 kHz.

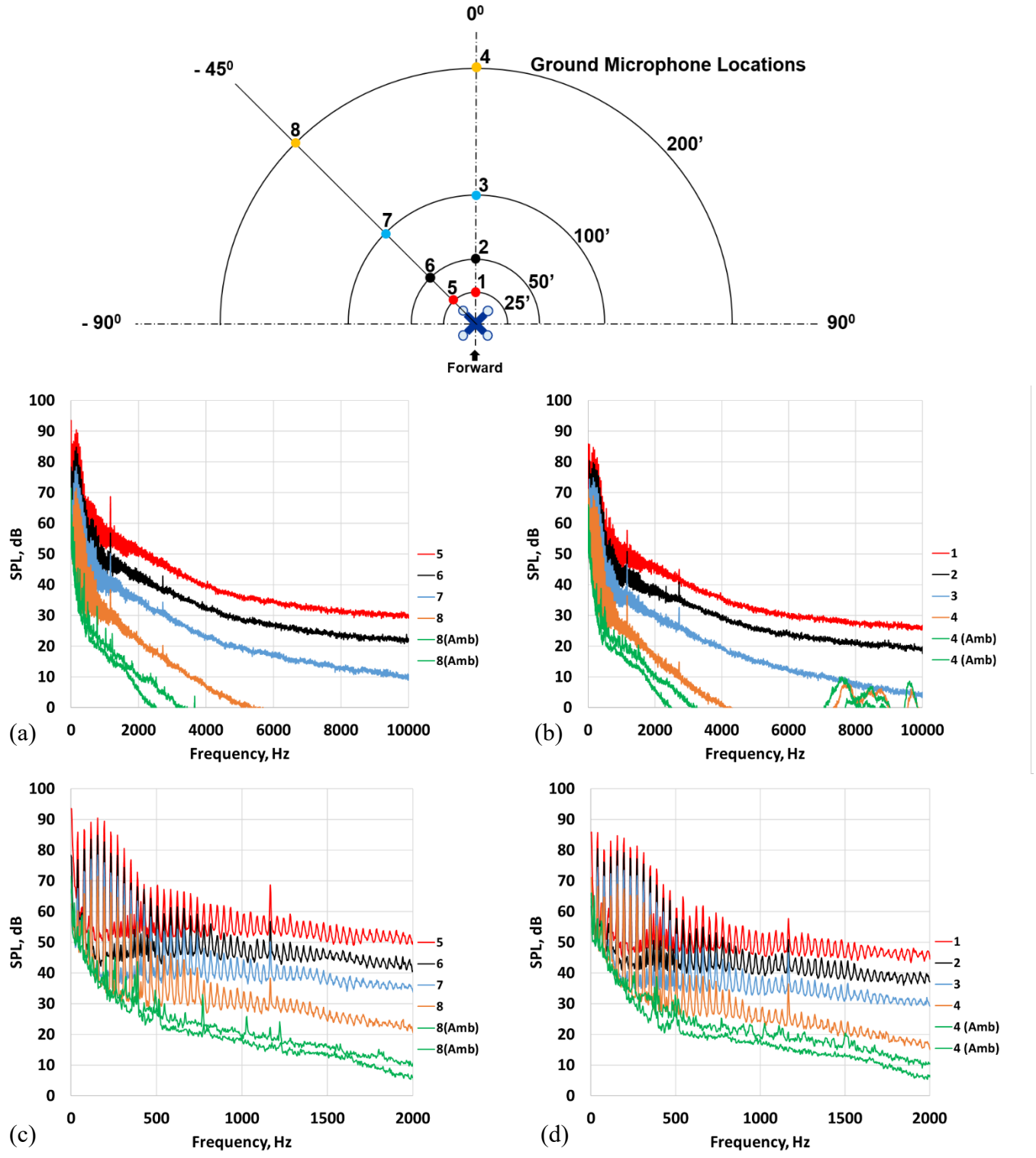

Figure 51.—SPL for left rear bottom rotor, 55 percent speed, run number 0037. (a) –45 degrees, 0 to 10 kHz. (b) 0 degrees, 0 to 10 kHz. (c) –45 degrees, 0 to 2 kHz. (d) 0 degrees, 0 to 2 kHz.

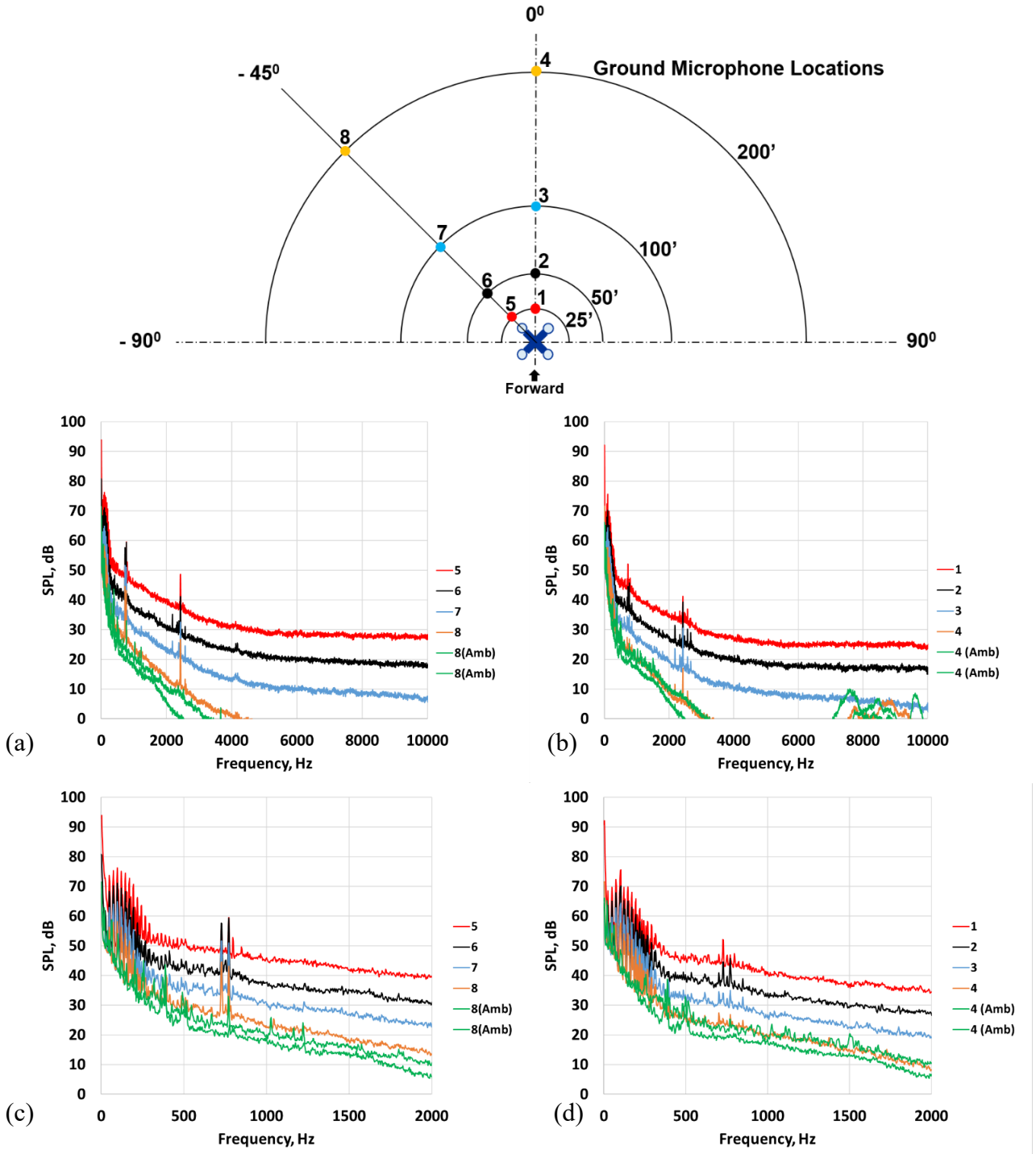

Figure 52.—SPL for left rear both rotors, 35 percent speed, run number 0038. (a) –45 degrees, 0 to 10 kHz. (b) 0 degrees, 0 to 10 kHz. (c) –45 degrees, 0 to 2 kHz. (d) 0 degrees, 0 to 2 kHz.

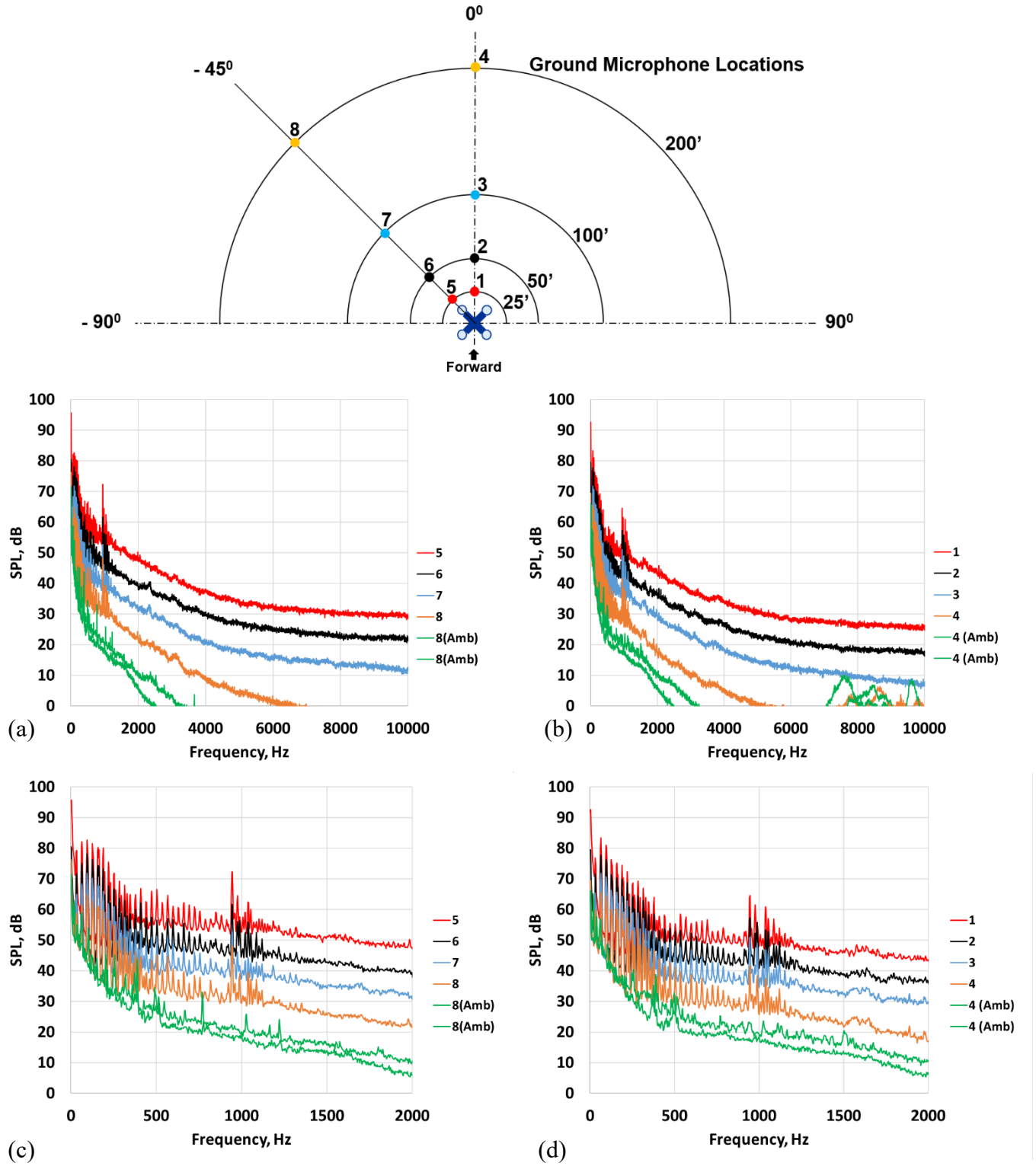

Figure 53.—SPL for left rear both rotors, 45 percent speed, run number 0039. (a) –45 degrees, 0 to 10 kHz. (b) 0 degrees, 0 to 10 kHz. (c) –45 degrees, 0 to 2 kHz. (d) 0 degrees, 0 to 2 kHz.

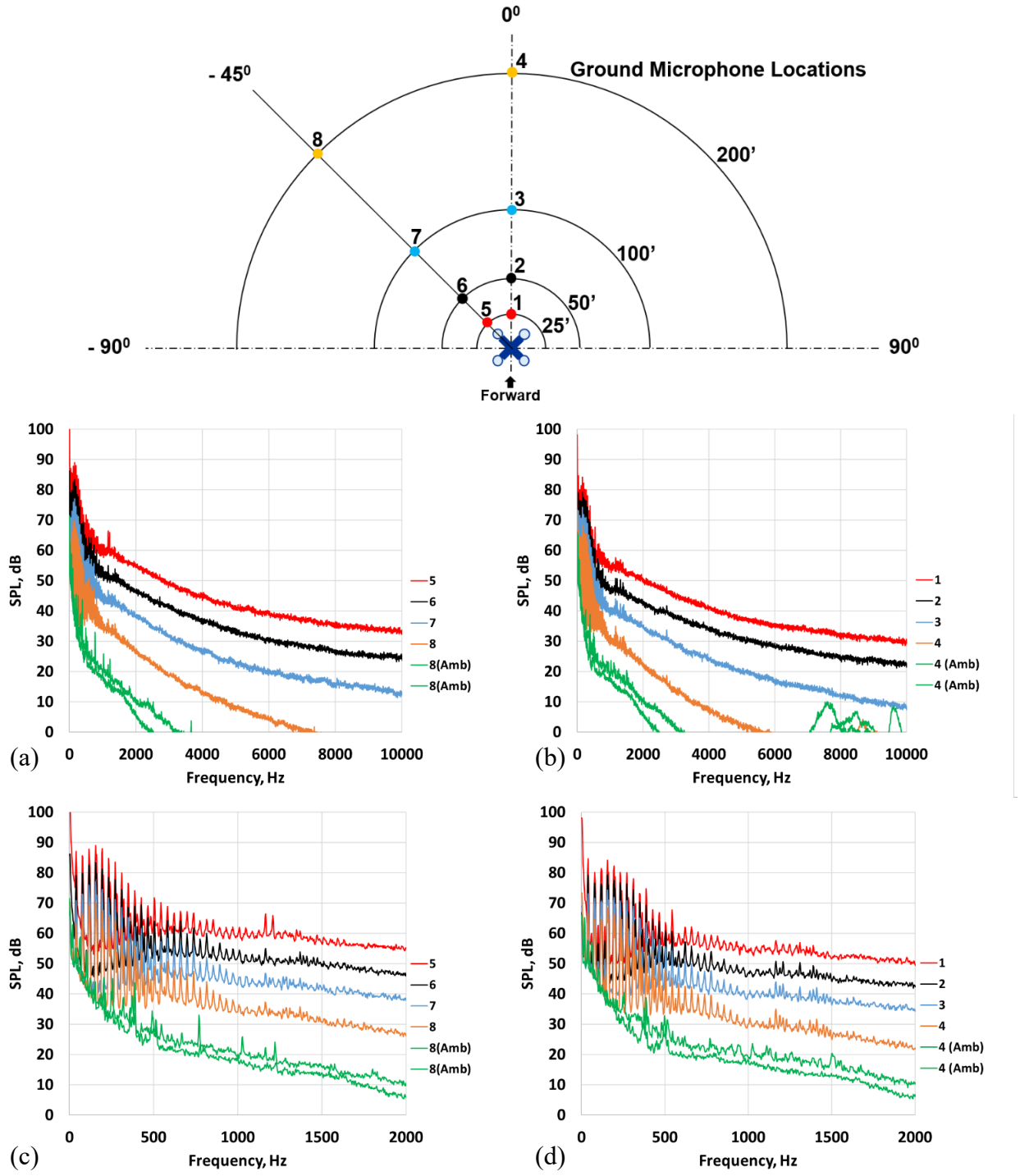

Figure 54.—SPL for left rear both rotors, 55 percent speed, run number 0040. (a) –45 degrees, 0 to 10 kHz. (b) 0 degrees, 0 to 10 kHz. (c) –45 degrees, 0 to 2 kHz. (d) 0 degrees, 0 to 2 kHz.

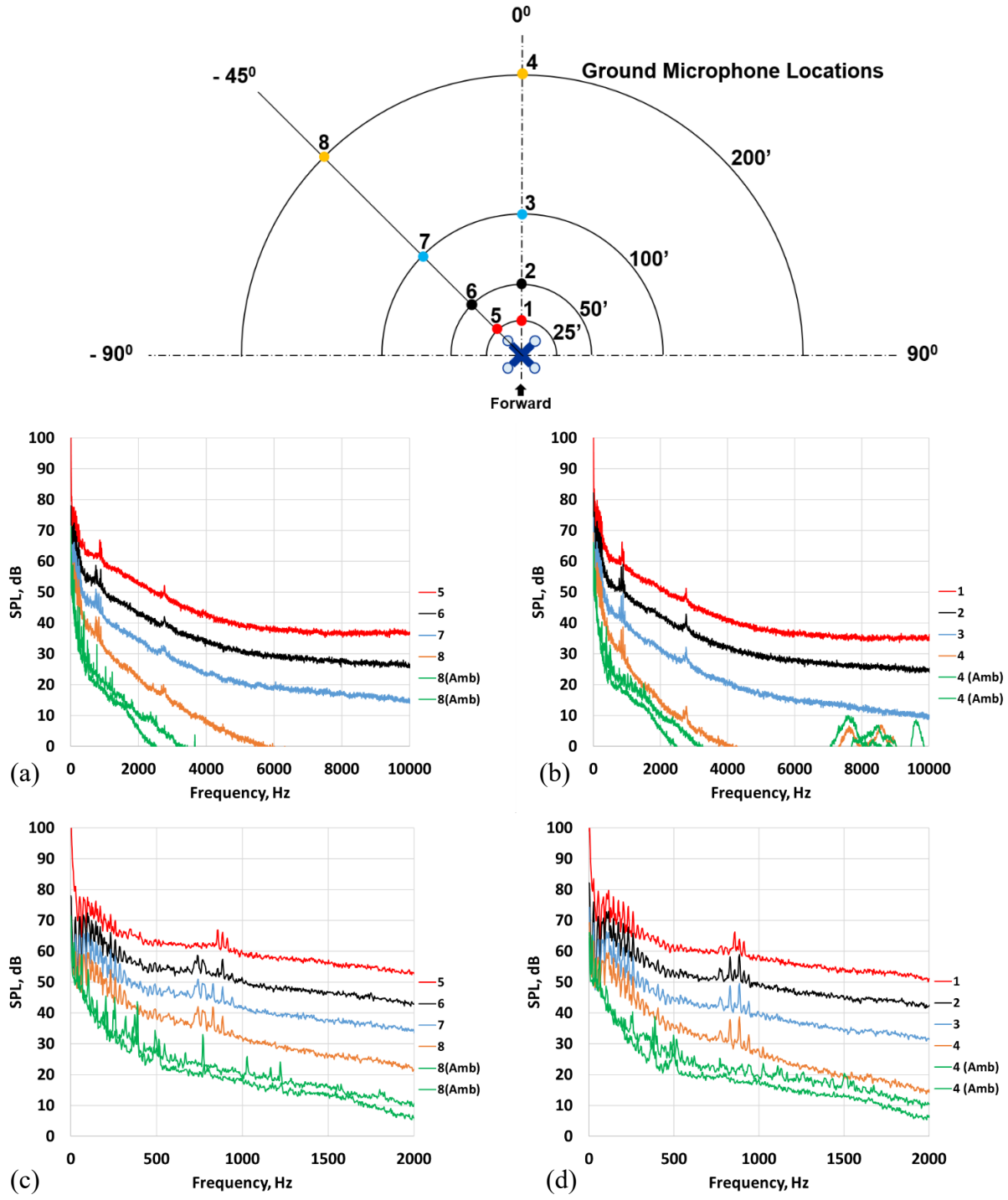

Figure 55.—SPL for all rotors, 35 percent speed, run number 0041. (a) –45 degrees, 0 to 10 kHz. (b) 0 degrees, 0 to 10 kHz. (c) –45 degrees, 0 to 2 kHz. (d) 0 degrees, 0 to 2 kHz.

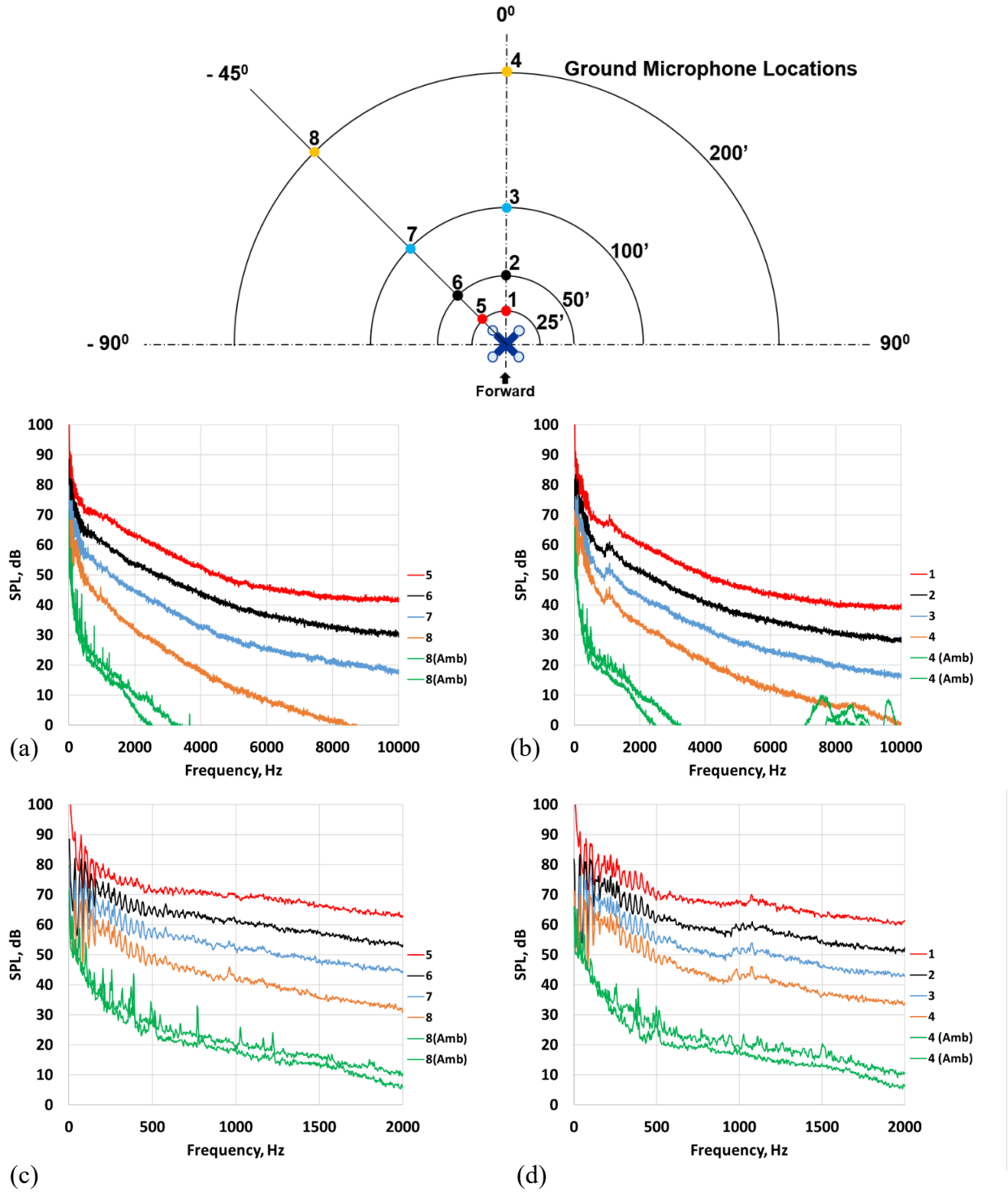

Figure 56.—SPL for all rotors, 45 percent speed, run number 0042. (a) –45 degrees, 0 to 10 kHz. (b) 0 degrees, 0 to 10 kHz. (c) –45 degrees, 0 to 2 kHz. (d) 0 degrees, 0 to 2 kHz.

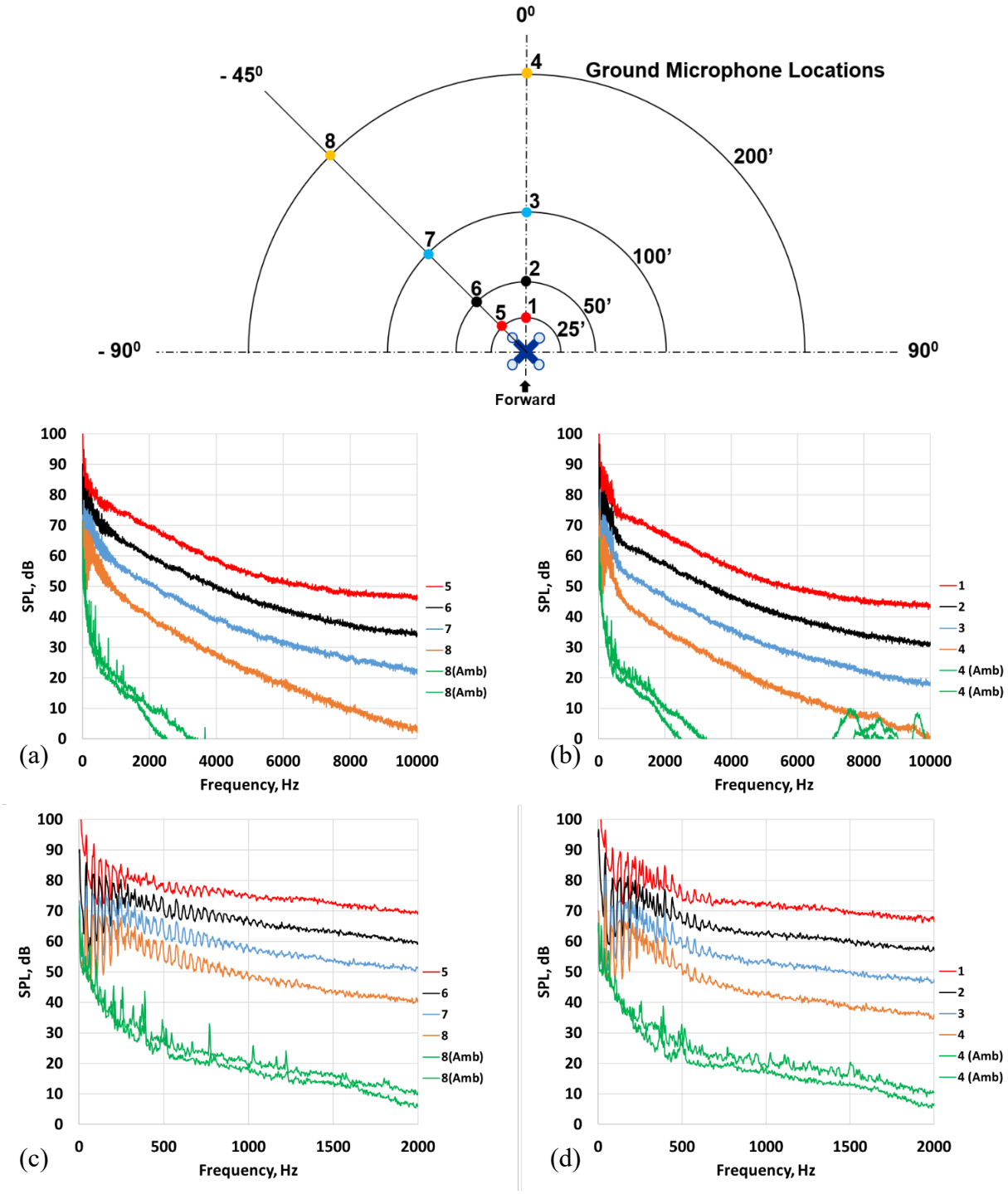

Figure 57.—SPL for all rotors, 55 percent speed, run number 0044. (a) –45 degrees, 0 to 10 kHz. (b) 0 degrees, 0 to 10 kHz. (c) –45 degrees, 0 to 2 kHz. (d) 0 degrees, 0 to 2 kHz.

Appendix C.—Overall Sound Pressure Level

The overall sound pressure level (OASPL) was computed from the narrowband spectra shown in Appendix B. Following ICAO standards (Ref. 6) for flyover noise evaluations, the 1/3-octave bands of interest are 17 through 40 corresponding to 50 Hz and 10 kHz center frequencies, respectively. To capture the entire bands, the narrowband spectra were summed from 44.7 to 11,220 Hz. A-weighting was added by adjusting the narrowband SPL at each frequency, f, as follows (Ref. 8):

$$SPL_A(f) = 2 + 20\log_{10}((12194^2 f^4)/((f^2+20.6^2)*SQRT((f^2+107.7^2)(f^2+737.9^2))*(f^2+12194^2)))$$

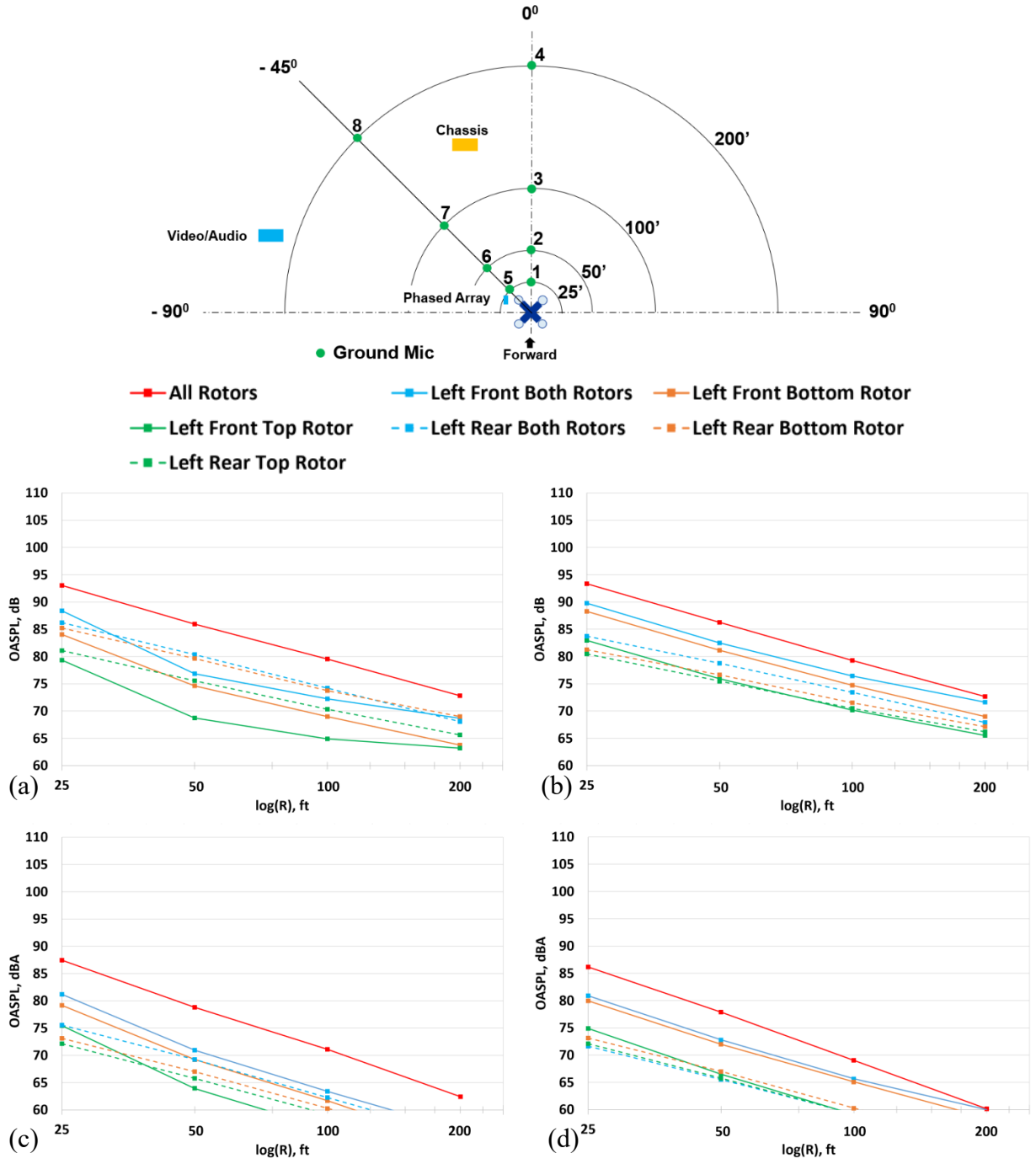

Figure 58.—OASPL, 35 percent speed. (a) –45 degrees, unweighted. (b) 0 degrees, unweighted. (c) –45 degrees, A-weighted. (d) 0 degrees, A-weighted.

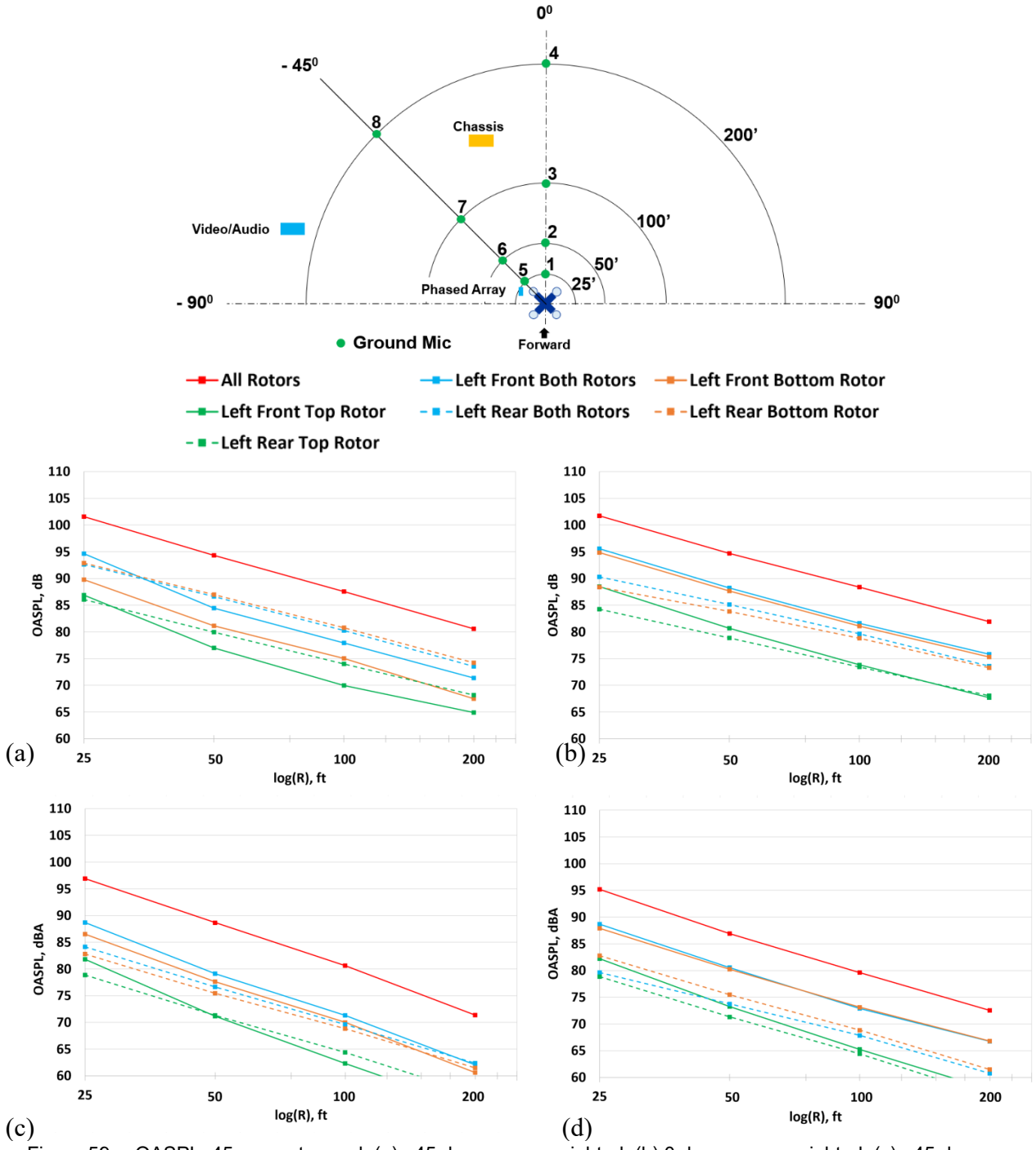

Figure 59.—OASPL, 45 percent speed. (a) –45 degrees, unweighted. (b) 0 degrees, unweighted. (c) –45 degrees, A-weighted. (d) 0 degrees, A-weighted.

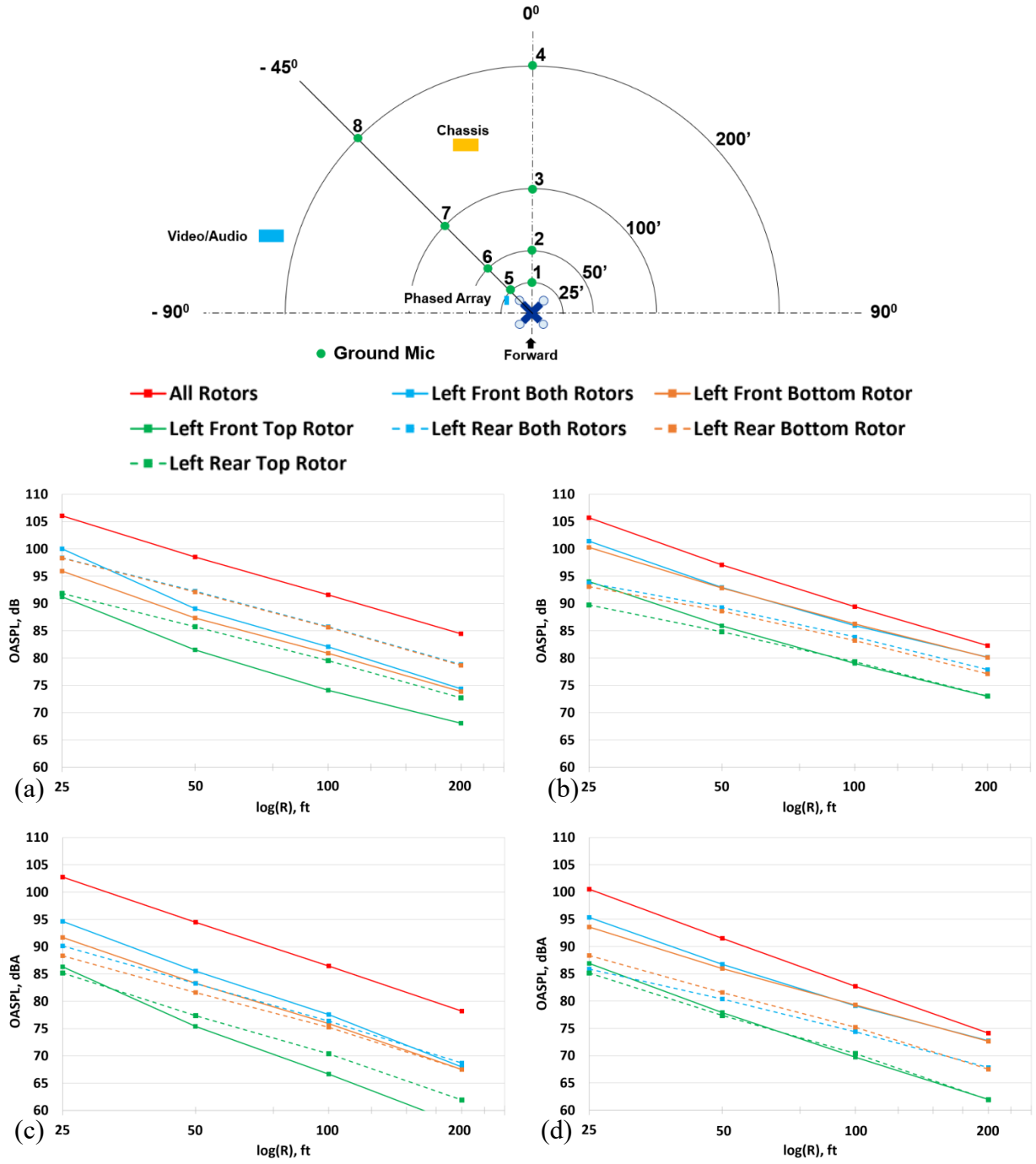

Figure 60.—OASPL, 55 percent speed. (a) –45 degrees, unweighted. (b) 0 degrees, unweighted. (c) –45 degrees, A-weighted. (d) 0 degrees, A-weighted.

References

1. Fast-forwarding to a Future of On-Demand Urban Air Transportation, Uber Elevate, October 27, 2016, https://www.uber.com/elevate.pdf. Accessed Feb. 17, 2021.
2. Rizzi, S.A., et al., Urban Air Mobility Noise: Current Practice, Gaps, and Recommendations, NASA/TP–2020-5007433, October 2020.
3. Dougherty, R., "BeamformX Reference Manual," Version 5, December 16, 2018, https://www.optinav.info/BeamformX_Manual_5002.pdf. Accessed February 22, 2021.
4. Weather Underground: https://www.wunderground.com/history/daily/us/oh/cincinnati/KLUK/date/2019-11-6. Accessed Feb. 23, 2021.
5. Huff, D.L. and Henderson, B.S.: Electric Motor Noise from Small Quadcopters: Part I – Acoustic Measurements, AIAA-2018-2952, June 2018.
6. Van Zante, D.E.: Progress in Open Rotor Research: A U.S. Perspective, Proceedings of ASME Turbo Expo, GT2015-42203, June 2015.
7. Environmental Technical Manual, Volume I, Procedures for the Noise Certification of Aircraft, International Civil Aviation Organization, Doc 9501-1, https://store.icao.int/en/environmental-technical-manual-volume-1-procedures-for-the-noise-certification-of-aircraft-doc-9501-1. Accessed April 27, 2021.
8. Electroacoustics – Sound Level Meters – Part 1: Specifications, IEC 61672-1:2013.